Abstract

Title of Thesis: Benthic Oxygen Production in the Choptank Estuary

Christopher Roberts Chick, Master of Science, 2009

Thesis directed by: Jeffrey Cornwell, Research Associate Professor
University of Maryland Center for Environmental Science

This study estimates the proportion of microphytobenthic (MPB) primary production to total primary production in the Chesapeake Bay using oxygen fluxes from sediment cores. Flux rates ranged from 6000 μmol O_2 m^{-2} h^{-1} in the light to -3800 μmol O_2 m^{-2} h^{-1} in the dark. Using this data, we developed multiple linear regressions using sediment grain type and depth to predict oxygen production seasonally. Using ArcMap software, we estimated summer average benthic daily net production to be 123 ± 962 mg O_2 m^{-2} d^{-1} between 0-3 meters and winter was estimated to be 152 ± 413 mg O_2 m^{-2} d^{-1}. For spring we had a weaker relationship, but benthic production was -257 ± 123 mg O_2 m^{-2} d^{-1}. A proportion of benthic to pelagic primary production was created, estimating that MPB provide approximately 12% of total primary production in the Chesapeake Bay.

Benthic Oxygen Production in the Choptank Estuary

By

Christopher Roberts Chick

Thesis submitted to the faculty of the Graduate School of the
University of Maryland, College Park, in partial fulfillment
of the requirements for the degree of
Master of Science
2009

Advisory Committee:
Dr. Jeffrey Cornwell
Dr. Todd Kana
Dr. Tom Fisher

Table of Contents

List of Tables

List of Figures

Introduction

In shallow water eutrophic systems, benthic autotrophic production is often limited by the available light at the sediment surface. Microphytobenthos (hereafter referred to as MPB) are an assemblage of unicellular eukaryotic algae and cyanobacteia that can contribute substantially to the carbon production and oxygen dynamics of benthic systems (Murray and Wetzel 1987; Moncreiff et al. 1992; Pollard and Kogure 1993). MPB, though patchy in small scale distribution, are ubiquitous where light is available, unlike sea grasses which are limited to distinct grass beds and are highly seasonal in their productivity. The abundance of shallow water sediments in estuaries, such as Chesapeake Bay (e.g. Kemp et al. 2005), suggests that contribution of MPB primary production in shallow waters can be significant depending on the amount of light reaching the sediment-water interface. In the upper millimeters of sediment, MPB oxygenate the sediments through photosynthesis and generate indirect affects on biogeochemical cycling as redox boundaries are pushed deeper into the sediment due to oxygen penetration (Rizzo 1990). MPB have also been observed to limit nutrient flux from sediments either through nutrient uptake or through indirect effects of sediment oxygenation (Sundback et al. 2000). In addition, Sundback et al. (1992) has shown that nutrient release from sediment under hypoxic and anoxic conditions is increased in light deprived sediments.

MPB excrete extracellular polymeric substances (EPS) which may facilitate diatom motility and serve as an adhesive that binds surface sediments. EPS limit sediment resuspension during high flow events and limit nutrient release to the water

column (Yallop et al. 1994; Lundvkist et al. 2007). Isotopically-labeled nutrients have been demonstrated to accumulate in EPS, indicating MPB play a role in sequestering water column nutrients in the sediments (Evrard et al. 2008).

MPB also function as a conduit by which sediment nutrients are cycled into higher trophic levels. MPB have been shown to be a major food source for nematodes, polychaetes, and other sediment heterotrophs. Montagna (1984) demonstrated the coupling between MPB and meiofauna through ^{14}C isotope studies. MPB grazing has been shown to be seasonally correlated with higher feeding in the warmer months and lower feeding in the cooler months (Pickney et al. 2003; Sullivan and Moncrief 1990). Some data suggest that meiofauna compete for limited MPB food availability, and that MPB abundance may control meiofauna populations (Carman et al. 1997). MPB grazing also indirectly stimulates increased MPB production by enhancing nutrient availability and thinning out current MPB populations for new growth (Kuhl et al. 1994). Overgrazing by herbivores and deposit-feeders can also reduce MPB standing stock and abundance (Montagna 1984; Miller et al 1996). In MPB colonized sediments, resuspension events sometimes occur and can provide a significant nutritional input for suspension feeders (Middelburg et al. 2000; MacIntyre et al 1996).

MPB in the Chesapeake Bay is primarily limited by benthic light availability with the highest rates of production reported during the warm summer months and lower rates during the late winter and spring (MacIntyre et al 1996 and references therein; Reay et al. 1995). MPB abundance has also been negatively correlated with turbidity and poor water quality (Facca et al 2002).

The habitat of MPB consists of littoral sandy beaches and mudflats, submerged aquatic vegetation beds and sub-tidal illuminated sediments. Sediment grain size has been shown to have a significant effect on MPB abundance. In the Chesapeake Bay, sandy sediments have higher MPB biomass and productivity (Rizzo and Wetzel 1985; Reay et al 1995). Silty sediments have been shown to impact the efficiency of herbivores and relieve grazing pressure (De Troch et al. 2006). In addition, silty sediments tend to be more responsible for high respiration rates than sandy (Reay et al 1996, Rizzo and Wetzel 1987).

In the 20th century, the Chesapeake Bay experienced greatly increased point and non-point source nutrient loading (Kemp et al. 2005). The almost complete loss of filter feeding by bivalves, the loss of aquatic macrophytes (SAV), the minimization of benthic microphytes, and the increased volumetric and areal coverage of anoxia negatively impacted the Chesapeake Bay. Despite efforts to limit nutrient inputs, restore SAV and restore oysters, it is clear that ecological degradation has not been attenuated. At some time, perhaps 40 years ago, the bay entered a new state in which the predominant nutrient cycling and productivity shifted from the benthos to the water column. Increased turbidity associated with eutrophication has stressed both macrophytic and microphytic production in bottom waters (Kemp et al. 2005).

MPB may play an important role in many ecosystems, though its quantitative role in the Chesapeake Bay is largely undocumented. Prior to eutrophication, MPB were a dominant part of the diatom assemblage in the bay (Cooper 1995). In many coastal ecosystems, benthic microalgae are important primary producers (Cahoon 1999) and mediate the production of phytoplankton and higher trophic levels through

their influence on ecosystem nutrient sequestration and cycling (i.e. Mallin et al. 1992; Moncreiff and Sullivan 2001; McIntyre et al. 2004). MPB can have a substantial effect on shallow water nutrient cycling, generally (but not always) limiting the process of denitrification and minimizing the efflux of nutrient elements to the water column (Sundback et al. 1991; An and Joye 2001; Risgaard-Petersen 2003).

Our knowledge of these shallow water processes in the Chesapeake Bay is limited to several field studies which have all involved analysis of O_2 flux by sediment core sampling (Rizzo et al. 1987; Murray and Wetzel 1987; Reay et al. 1995; Kemp et al. 1999; Holyoke 2008). No studies within the Chesapeake Bay have examined MPB production using spatial resolution software or have estimated regional or bay- wide levels of sediment-based MPB production (aside from the limited approach in Fear et al. 2004). The advantage of the GIS approach is that it provides some quantifiable power of prediction over different spatial fields as long as they share attributes with the sampling location.

The goal of this study is to determine the importance of MPB relative to total primary production in the Chesapeake Bay. Based on previous findings in Kemp et al. (1999), ***we hypothesize that MPB will contribute highly to total primary productivity in areas with water depths ≤ 3 meters, but for the Chesapeake Bay MPB will contribute no more than 10% of total primary productivity as estimated by Kemp et al (1999)***. However the Kemp et al. data were based on few benthic measurements and had a minimal spatial component. Below 3 meters, light conditions generally did not permit abundant MPB biomass.

In this study, we test this hypothesis using from sediment cores and sampling site measurements to construct a spatial map to estimate MPB primary production in the Chesapeake Bay. Benthic sediment cores were retrieved from euphotic sediments in the Choptank River and used to generate relationships between biotic and abiotic variables, such as light, chl *a* concentration, sediment grain size and oxygen flux rates. By comparing differences in the rates of oxygen flux between cores we were able to determine which factors in the Chesapeake Bay have the most impact on MPB production and used them to predict production over a portion of the Chesapeake Bay. Using these predictions, we estimated how MPB gross and net primary production changes seasonally in the Chesapeake Bay.

Data relationships were used to generate multiple linear regressions which became GIS-based models to provide estimations of O_2 flux across areas of the Chesapeake Bay. A limitation of this approach is that the value of the prediction is related to size of the r^2 value connected to the regression.

Light has been demonstrated to be a main limiting factor in MPB production in estuaries with euphotic sediments (e.g. Kemp et al. 2005), but secondary environmental variables may have a significant impact. In this study, it was impractical to use irradiance as a variable in the spatial map, due to the unavailability of spatial irradiance data. As a result, depth was chosen as a proxy to irradiance, as bathymetric maps are readily available and can provide a useful proxy for light values. The other statistically significant variable used in generating the spatial map was sediment grain size expressed as percent sand. Previous studies have shown

sediment grain size to be a significant factor in MPB primary productivity (Rizzo and Wetzel 1985).

This study estimates MPB productivity from a total of 13 sampling dates over a period of a year. MPB communities are characterized by high spatial and temporal variability, and this presents challenges in generating estimates of MPB abundance. Chlorophyll *a* (Chl *a*) concentrations, on a cm^2 scale, can vary 3 fold over a 50x50 cm area depending on local conditions (Varela and Penas 1985). Moreover, Miles and Sundback (2000) have suggested that sampling less than once a month introduces at least 40% error into an MPB estimate and that minimum sampling should be at least 4 days out of a month. As a result, this study's ability to estimate temporally contiguous change is limited and relies on seasonal data to define MPB productivity by season. To account for the high variation of MPB abundance, this study employed increased replication at each sampling site.

Study Site

Study sites included the mainstem Choptank River, referred to as the Horn Point site (HP), La Trappe Creek (LTC) and Fishing Bay (FB), all sub-estuaries of the Chesapeake Bay (Figure 1). The Choptank River estuary covers ~ 300 km^2 with a mean water depth of 3.6 meters and is characterized by high algal biomass derived from both non-point and point N and P inputs. The Choptank River is 26 meters deep at its maximum and is separated at its mouth from the Chesapeake Bay by a sediment sill (Fisher et al. 2006). The transect site at Horn Point Laboratory was located on a north-facing shoreline, with water depths ranging from 0 to 3 meters. This site also

had less light attenuation than LTC and FB. The LTC site is a highly turbid creek environment on the north side of the Choptank River, draining mostly agricultural land; LTC is characterized by high resuspended sediment concentrations and high algal biomass, resulting in high light attenuation and summer hypoxia (Holyoke 2008). FB is a large shallow habitat which experiences high turbidity year round. A three site transect of cores to depths up to 3 meters was collected. FB is surrounded by brackish and oligohaline marshes and much of the upstream land use is agricultural.

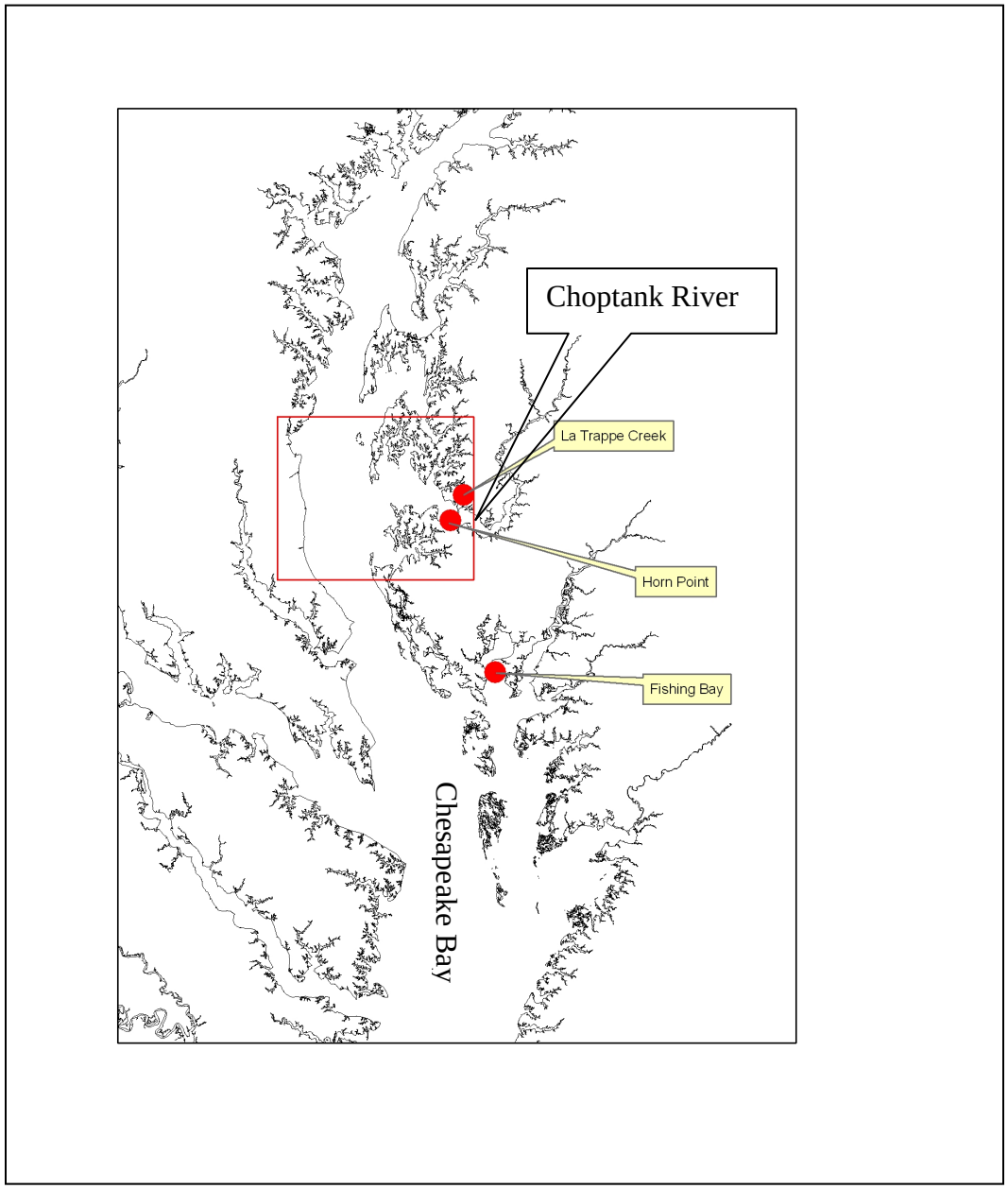

Figure 1. Transect sites are indicated with red dots, the red box denotes the study area used for GIS-based spatial extrapolation.

Methods

This study was conducted between June 2005 and September 2006. Cores were collected from the 3 transect sites with 3 stations per transect. At the HP site, MPB production was measured 7 times. LTC and FB were each sampled 3 times during the year. During each sampling, cores were obtained from transects consisting of 0-1m, 1-2m, and 2-3m deep sampling stations. In addition, a 9m station was sampled in the mid-Choptank River to provide an aphotic reference site. Bottom sediments at this site were collected using a box corer (Owens 2009). Sampling dates are shown in Table 1.

Table 1. List of sampling locations and dates.

Sampling	Date	Location
HP1	6/7/2005	HP
HP2	7/24/2005	HP
HP3	11/15/2005	HP
HP4	1/24/2006	HP
HP5	3/8/2006	HP
HP6	5/9/2006	HP
HP7	6/30/2006	HP
LTC	8/30/2005	LTC
LTC2	2/7/2006	LTC
LTC3	6/7/2006	LTC
FB1	8/16/2005	FB
FB2	3/30/2006	FB
FB3	8/2/2006	FB

Cores were collected using a pole corer with 7 cm diameter in transparent acrylic tubes. Each tube contained ~15 cm of sediment and ~15 cm of overlying water. Bottom water was collected with a diaphragm pump; on most dates, the water was inline filtered using with a 0.5 micron filtering cartridge. Sediment and surface

illumination was measured using a LI-COR 2π photosynthetically active radiation (PAR) sensor. The attenuation coefficient, *k*, was calculated using the water attenuation equation shown here;

$$k = \frac{\ln(\frac{E_0}{E_Z})}{Z}$$

where E_0 is the irradiance at the surface and E_z is the irradiance at depth, and Z was the depth of the sensor. Light conditions were not normalized to the sunny day conditions.

On most dates, a Secchi disk was also used as a secondary light attenuation measurement Depth was recorded by weighted marked rope, conductivity, temperature and depth sensor (CTD) lowered from the boat.

Upon returning to the laboratory the core tubes were placed in cylindrical tanks with internal separations for each depth sampling station. A walk-in environmental chamber was used to maintain the temperature and irradiance at near-*in situ* conditions. Core water columns and replacement water collected from the sampling station were bubbled overnight to ensure oxygen saturation and thermal equilibrium between sediment and water. Three replicate cores from each sampling station were incubated along with an empty tube containing only station water. This water-only in each treatment served as a blank for measuring pelagic processes. The next morning magnetic stirring tops were placed on the tubes, followed by ~ 8 hours of incubation split between dark and illuminated conditions.

A fluorescent light bank (Teklight T5 photobank with eight tubes) was used to simulate *in situ* light conditions with perforated fiberglass shade cloths to match field

illumination. The maximum PAR produced by the light bank was ~300 μmol m^{-2} s^{-1} at the surface of the cores and PAR was reduced to simulate deeper *in situ* stations using layers of neutral density screening. *In situ* irradiances higher than 300 μmol photons m^{-2} s^{-1} could not be replicated in these experiments. At 30-60 minute intervals, 10 mL water samples were collected in glass-stoppered vials for oxygen concentration analysis. Samples were immediately preserved with 10 uL of a 0.29 mol L^{-1} HgCl solution. An additional 20mL was also collected to measure the inorganic nutrient flux. Replacement water was gravity fed into the flux cores.

At the end of the flux experiment, two sediment chlorophyll a (chl *a*) samples were taken from the surface sediment of each core using the top 1 cm of a 10mL syringe. Chl *a* samples were stored frozen and analyzed < 6 months after collection. Chl *a* samples were thawed and extracted in 90% acetone after extraction at 0°C for 24 hours, with final analysis via HPLC (Van Heukelem et al. 1994). The top 2 cm of sediment from one core from each site was removed for sediment grain size analysis using a Sedigraph (Coakley et al. 1991), and a wet sediment sample was collected for determining percent water after drying at 65°C. The height of the water column and sediment was recorded to determine water volume.

Oxygen samples were taken at regular intervals during the light and dark incubation periods. Sampling intervals were shorter during incubations for highly productive cores. This was necessary, typically during the summer, to minimize O_2 supersaturation. Oxygen samples were killed with $HgCl_2$ solution to halt biologically mediated gas exchange in the water, and samples were kept at 10 ^{o}C.

O_2 concentrations were measured using a membrane inlet mass spectrometric (MIMS) technique (Kana et al. 1994). By using argon concentrations as a comparison and assuming it stayed stable over time, oxygen to argon ratios were used to precisely measure O_2 concentration changes. The MIMS technique offered two main advantages: 1) a precision of ~ 0.05% and 2) the capability to preserve samples for later analysis (Kana et al 1994). Oxygen flux rates in the blank cores were subtracted from the sediment core rates to account for the water column effect on respiration and primary productivity. Instrument drift was corrected using repeated analysis of temperature/gas equilibrated standards (Kana and Weiss 2004).

Time courses of oxygen concentration are shown for a sample incubation of Choptank River cores (Figure 2). The dark and light flux rates were each calculated via linear regression using 4 data points from each core; one data point was shared at the point of light/dark transition. The 3 replicate rates were then averaged to represent the O_2 flux rate from each point in the transect. For a given set of replicates, the standard deviation of concentration tended to increase with increasing time. Shallower sites tended to shift to positive rates in the light while deeper sites experienced a slight decrease in negative O_2 flux. Photosynthesis is indicated by a difference in sequential dark and light rates (an increase in O_2 flux).

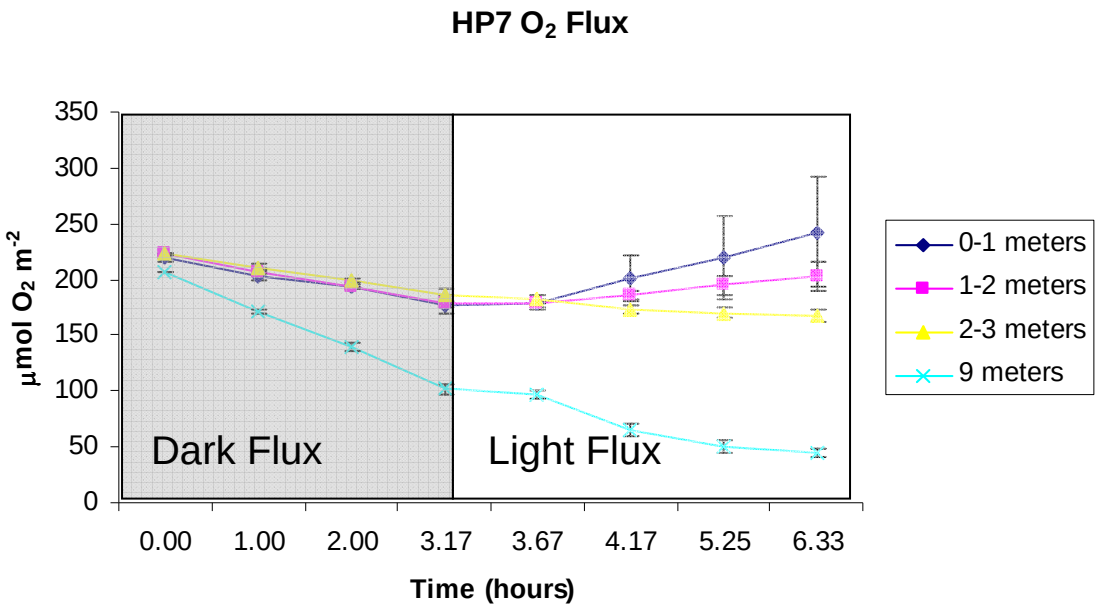

Figure 2. HP O_2 fluxes. A time course of averaged cores from the HP7 sampling date. Both the light and dark regressions included the middle time point. Initially, cores were incubated in the dark and have correspondent negative rates. After the first four time points, light was added. When light was turned on core O_2 rates change depending upon photosynthesis.

As figure 2 shows, time dependent concentration changes for each sampling depth generated an hourly O_2 flux rate for the dark and the light. These rates were then used to calculate hourly and daily net and gross O_2 production values.

Hourly net O_2 consumption was taken as the unaltered light O_2 flux. This value, without adulteration, represents the difference of hourly light O_2 consumption and photosynthesis at an hourly rate. In calculating hourly gross O_2 production, the assumption was made that the dark flux rate was constant and persists in the light as the background O_2 consumption. Thus, subtracting the negative dark hourly O_2 flux values from the light hourly O_2 flux values resulted in compensation for background O_2 consumption plus positive O_2 flux.

Daily gross O_2 (photosynthetic) production rates were obtained by the difference between hourly dark rates and hourly light rates and multiplying by the hours of daylight on the sampling day. Again like the hourly gross rate, the assumption is that the dark rate generated O_2 consumption rate remained constant throughout the day and night. Daily respiration was obtained by multiplying the hourly dark rate by 24 hours. Net daily oxygen flux was calculated by multiplying the hourly dark rate by 24 hours to represent the background heterotrophic activity and then adding the daily gross value to this daily respiration value. During the core incubations, no accounting was made for the transitional waxing and waning irradiances of morning and evening. Simulated night-time ended immediately and daylight began immediately.

In order to determine predictive variables for net and gross O_2 production a series of multiple linear regressions were performed using depth, chl *a*, PAR, attenuation coefficient, and sediment type. The resultant regressions showed that both irradiance and depth combined with percent sand produced significant relationships to predict benthic O_2 production. However, light was not an ideal variable with which to generate a map, as the light data available did not have a sufficient spatial component, but spatial depth data was available in bathymetry. Thus, depth was used in place of irradiance along with percent sand as a variable to predict O_2 production in the multiple linear regressions.

The equations generated from the regressions were input into the attribute table of ArcMap 9.2 and used to predict seasonally specific O_2 production values. An ArcMap polygon file of the CB depicting sediment grain size and a raster bathymetry

map were obtained from Maryland DNR (Jeff Halka, unpublished data). The sediment grain size map was generated using 5cm sediment cores from surficial sediments collected in 1976-1984. Samples were taken along shore-perpendicular transects located approximately 1 km apart. Thus, the sediment grain size data has a resolution of 1km. Using ArcMap 9.2 the raster file and the polygon file were merged to combine the attributes over a shared spatial field. The equations predicting gross and net O_2 production were input into the attribute table of a shapefile in ArcMap, where they were used to estimate areas of production within an area of shallows 0-3 meters deep in an area of approximately $2.6x10^8$ m^2.

Results

Salinity and temperature mesurements at the Horn Point (HP) site were similar to the nearby Chesapeake Bay monitoring data station (Figure 3). Temperatures ranged from 28^o C to 5^o C. Salinity ranged from 7.9 to 13.3 ppt with no significant relationship between salinity and temperature.

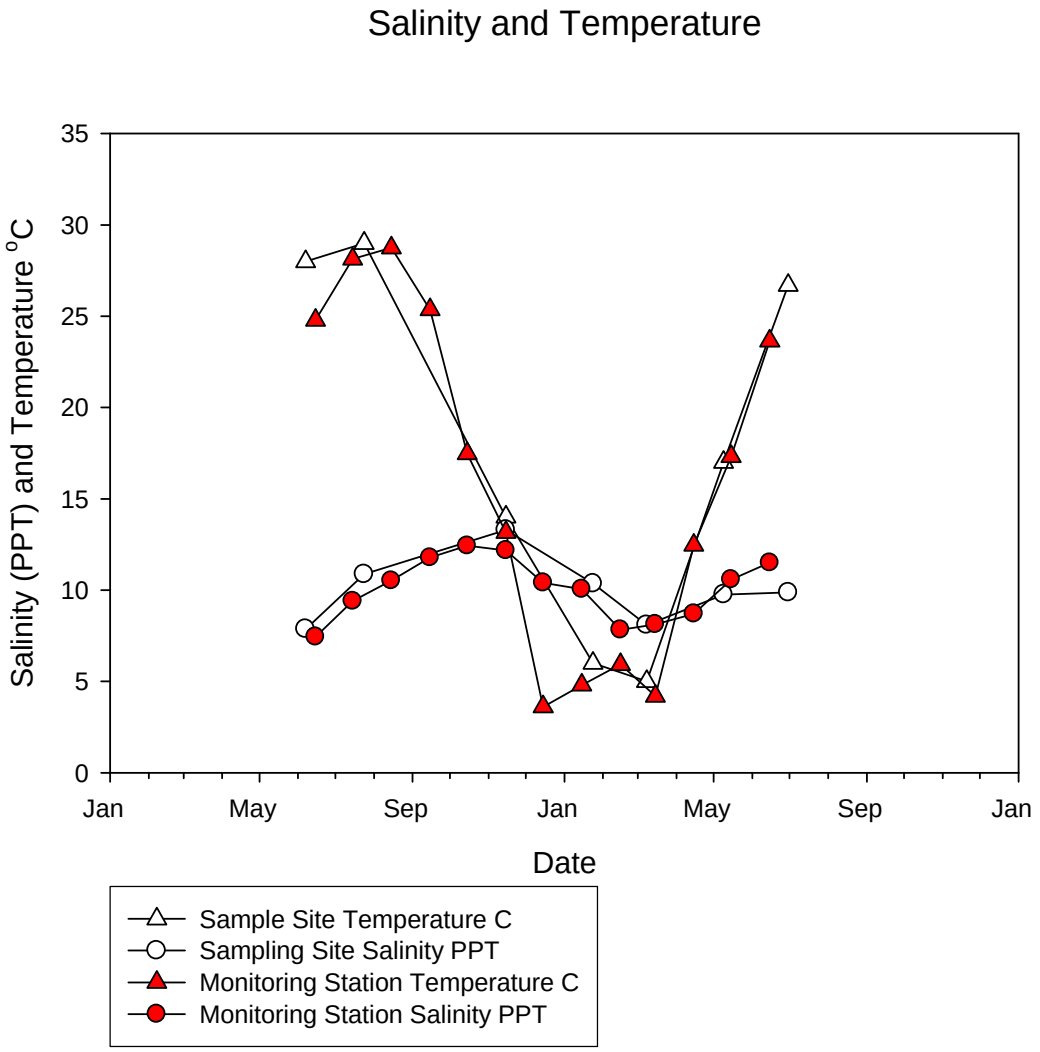

Figure 3. Salinity and temperature from the Horn Point site as measured by CTD at the sampling depth compared to monthly salinity and temperature from station ET5.2 from the Chesapeake Bay Observing System.

Surficial chlorophyll *a* concentrations (chl *a*) were similar to other MPB measurements reported for shallow water Chesapeake Bay sediments (Rizzo and Wetzel 1985). Chl *a* mg m^{-2} values were much higher at HP than at the other tributary sites (Figure 4). At HP, chl *a* was the highest in the summer with shallow depths having the highest chl *a* values. The average yearly chl *a* concentration was 117 mg m^{-2} at 0-1 m depth, 60 mg m^{-2} at 1-2 m, and 20 mg m^{-2} at 2-3 m. HP chl *a*

values from each sampling depth were significantly different ($P<0.05$). At, LTC, the average at 0-1 m chl *a* was 14 mg m^{-2},with average concentrations of 11 mg m^{-2} and 8 mg m^{-2} at 1-2 and 2-3 m respectively. At FB the average at 0-1, 1-2 and 2-3 m was 11 mg m^{-2}, 7 mg m^{-2} and 5 mg m^{-2} respectively. The highest observed value of chl *a* during this study was 199 mg m^{-2} during the summer at HP in the 0-1 meter range. The lowest was 2 mg m^{-2} during the summer at LTC. The chl *a* values for summer were significantly higher than those for spring and fall ($P<0.05$) Spring and winter chl *a* values were not significantly different from each other ($P<0.05$).

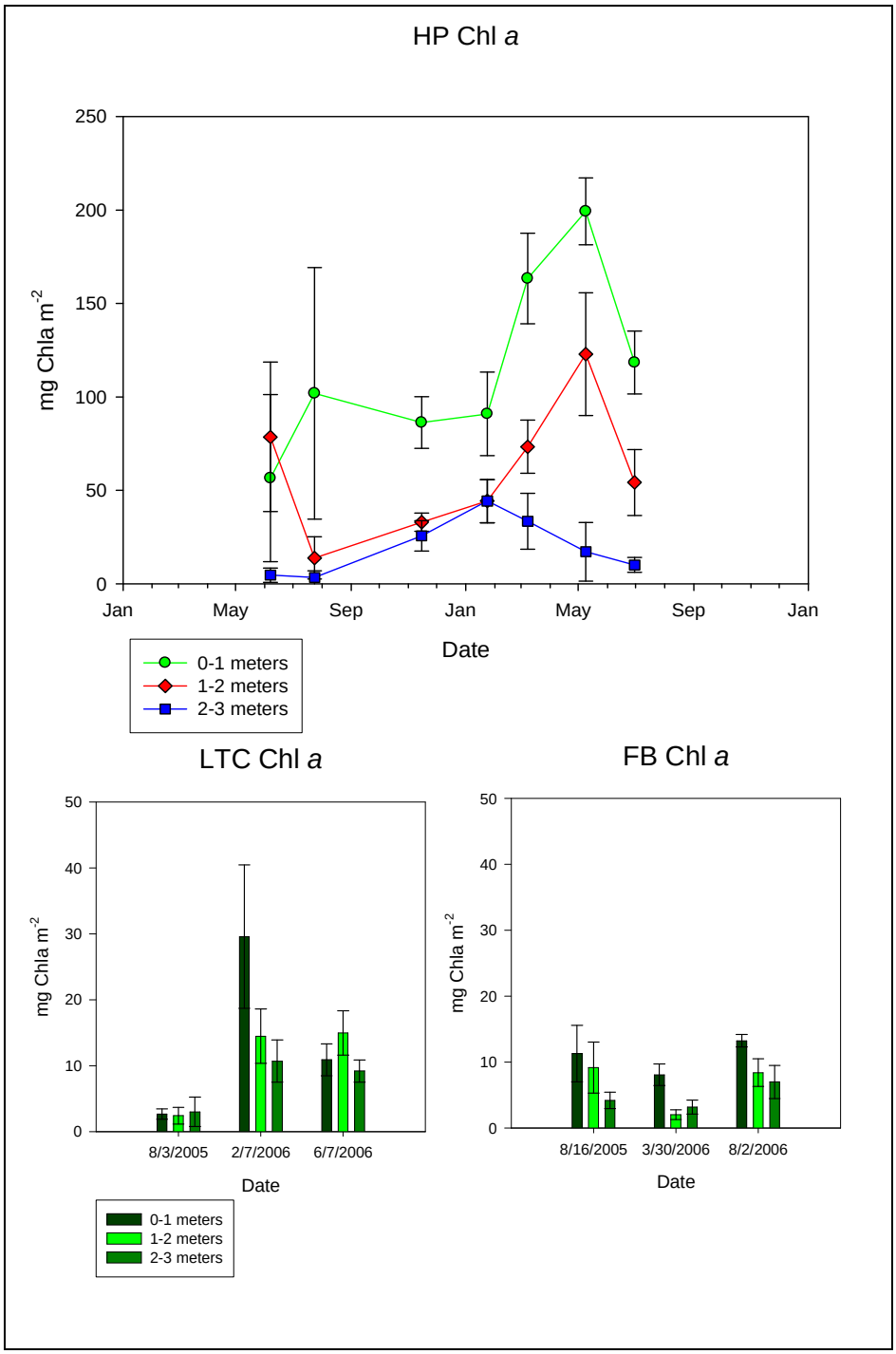

Figure 4. Chl *a* data for all times and dates as measured by HPLC from each sample site. Two chl *a* samples were collected from each core.

Sediment grain size distribution varied between sites. HP sediment was largely composed of sand at all water depths (Table 2). LTC sediment composition was primarily clay but has sizable fractions of larger particles. FB sediment was variable with depth with a large fraction of sandy sediment in shallower depths, and high silt and clay from the deepest site. Percent sand was the only grain type that produced a significant correlation with O_2 flux ($P<0.05$).

Table 2. Sediment grain composition from 5cm sediment samples. Sand was defined as 4-0 phi, silt as 4-8 phi and clay as 8+ phi.

Sites	Depth m	%Sand	%Silt	%Clay
HP	1	96.3	0.6	3.0
HP	2	97.1	2.5	0.4
HP	3	92.2	2.6	5.2
LTC	1	24.3	30.6	45.1
LTC	2	9.9	32.2	57.9
LTC	3	20.9	24.3	54.8
FB	1	40.8	na	na
FB	2	89.7	4.2	6.0
FB	3	6.9	45.1	47.9

In this study, sediment type (sand or silt-clay) had a correlation with MPB biomass only during the summer season, whereas during other seasons, sediment type had no significant relationship with chl *a* concentration. There was also a cross-site significant relationship ($p<.001$, $r^2 = 0.14$) between depth and chl *a*; limiting the data analysis to the HP site improved the relationship ($p<0.001$, $r^2 = 0.53$).

There were significant differences in O_2 flux rates in light between sampling depths at HP. Under illumination, shallow and mid depth sites at HP had significantly higher positive flux rates than the deeper sites ($P<.05$; Figure 5). During the dark fluxes, shallower water O_2 flux rates were not significantly different from those from deeper environments; thus, sediment respiration was generally similar at all HP

depths. However, light O_2 flux rates were much higher in shallow depths, particularly in warmer months. The deepest (>7 meters) site consistently showed negative fluxes which became more negative in the warmer months; this pattern is consistent with previous studies at this site (Owens 2009). Collectively and individually, the light O_2 flux values were significantly different from those measured during the dark treatment using the Mann Whitney Rank Sum Test ($P<.001$).

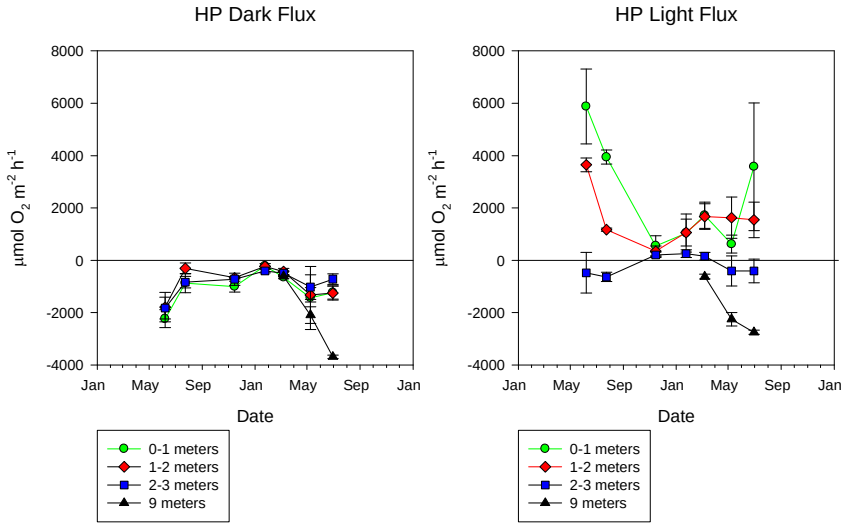
HP Dark Flux
µmol O2 m-2 h-1
8000
6000
4000
2000
0
-2000
-4000
Jan
May
Sep
Jan
May
Sep
Jan
Date
0-1 meters
1-2 meters
2-3 meters
9 meters

HP Light Flux
µmol O2 m-2 h-1
8000
6000
4000
2000
0
-2000
-4000
Jan
May
Sep
Jan
May
Sep
Jan
Date
0-1 meters
1-2 meters
2-3 meters
9 meters

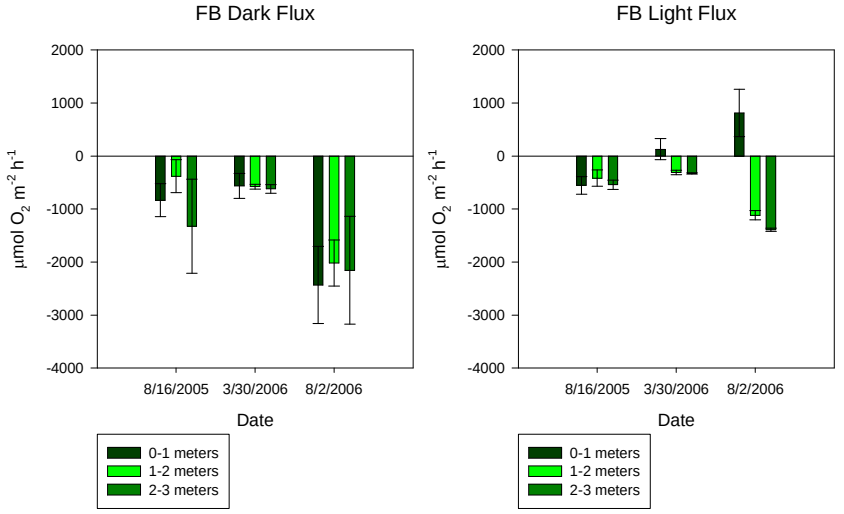
FB Dark Flux
µmol O2 m-2 h-1
2000
1000
0
-1000
-2000
-3000
-4000
8/16/2005
3/30/2006
8/2/2006
Date
0-1 meters
1-2 meters
2-3 meters

FB Light Flux
µmol O2 m-2 h-1
2000
1000
0
-1000
-2000
-3000
-4000
8/16/2005
3/30/2006
8/2/2006
Date
0-1 meters
1-2 meters
2-3 meters

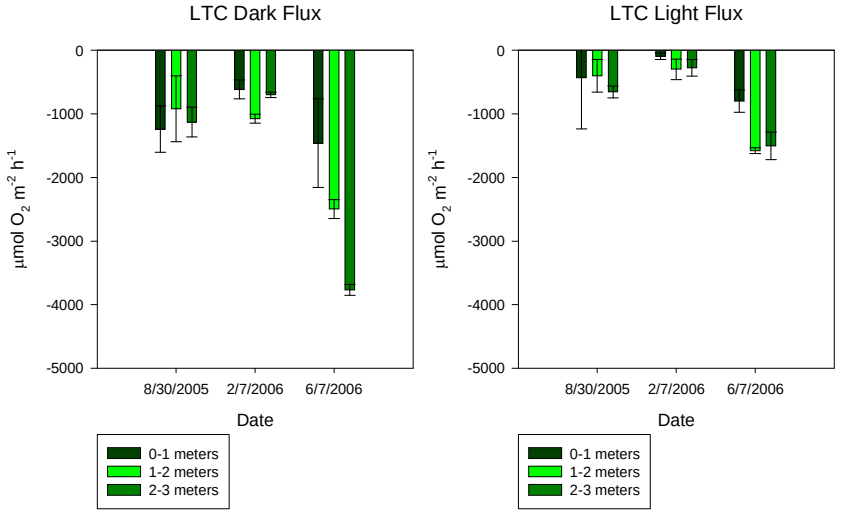
LTC Dark Flux
µmol O2 m-2 h-1
0
-1000
-2000
-3000
-4000
-5000
8/30/2005
2/7/2006
6/7/2006
Date
0-1 meters
1-2 meters
2-3 meters

LTC Light Flux
µmol O2 m-2 h-1
0
-1000
-2000
-3000
-4000
-5000
8/30/2005
2/7/2006
6/7/2006
Date
0-1 meters
1-2 meters
2-3 meters

Figure 5. Dark and light flux results from HP, FB, and LTC. At HP the deepest site was 7-9 meters and was only sampled during the final three sampling times. Lines are to guide the eye not to suggest continuity of data. Negative fluxes indicated oxygen flux into the sediment; positive fluxes indicate a flux out of the sediment.

FB dark oxygen fluxes were similar in magnitude (but not significantly) to HP fluxes. The FB light fluxes ranged between -380 to -2434 μmol O_2 m^{-2} h^{-1}(Figure 5). The light fluxes had showed a positive flux above 0-1 meter station during the March and second August sampling dates, but otherwise were negative. Light and dark flux rates were significantly different from each other ($P<0.05$), and the second August dark flux rates had significantly higher absolute magnitude than dark flux rates from the other two months ($P<0.05$). The highest positive and negative flux rates were both observed during the second August sampling date.

All O_2 flux rates at LTC were negative both in the light and dark light regimes, though slightly less negative in the light (Figure 5). The most negative O_2 dark flux rates at LTC occurred in June of 2006 at the deepest site, and the least negative dark flux rates were in February at the shallow site. In the light, the lowest negative flux was at the shallow site and the highest negative flux was in June in the deepest site.

The LTC cores all displayed fluxes consistent with Holyoke's (2008) observations. However, the light treatment cores had less oxygen uptake, indicating the presence of photosynthesis. In this study, the June data at LTC had the most negative average dark O_2 uptake of -3800 μmol O_2 m^{-2} h^{-1} followed by the 7m site at HP in June 2006 (-3600 μmol O_2 m^{-2} h^{-1}). The two highest average positive O_2 fluxes in the light were measured at HP in June and July 2005.

Hourly net and gross oxygen production were estimated from the light and dark oxygen fluxes as follows:

1) **Hourly Net rate** = measured oxygen fluxes (μmol m^{-2} h^{-1})

2) **Hourly Gross rate** = light rate (μmol m^{-2} h^{-1}) – dark rate (μmol m^{-2} h^{-1}).

The hourly gross O_2 production presumes that microbial/chemical oxygen uptake determined under dark conditions remains the same under illumination.

The data points which are shown at 600 μmol m^{-2} s^{-1} in Figure 8 and 9 are cores which were incubated in outdoor natural light due to issues with the incubation chamber.. The remainder of all cores in the study were incubated at *in situ* irradiances with a maximum of 300 μmol m^{-2} s^{-1} under artificial light conditions.

There was a significant relationship between environmental chamber PAR and hourly gross O_2 flux and hourly net O_2 flux at HP on some sampling dates, although few individual transects displayed significant relationships between O_2 production and PAR ($P<0.05$) (Figure 8; Table 3). Among all the data as a group annually, there was a significant relationship between PAR and productivity ($P<0.05$) (Figure 6), however the r^2 value was low indicating that very little of the O_2 flux trend variability could be solely attributed to PAR (Figure 6). Taken as a group, the HP transects display a much stronger significant relationship between PAR and hourly net and hourly gross O_2 flux as shown in Figure 8. Although, many of the r^2 values are very high in table 5, the few data points do not allow for a significant relationship between hourly net and gross O_2 flux and PAR within most of the individual sampling

transects. For cores with three transect points, r^2 needed to be over 0.99 to attain significance.

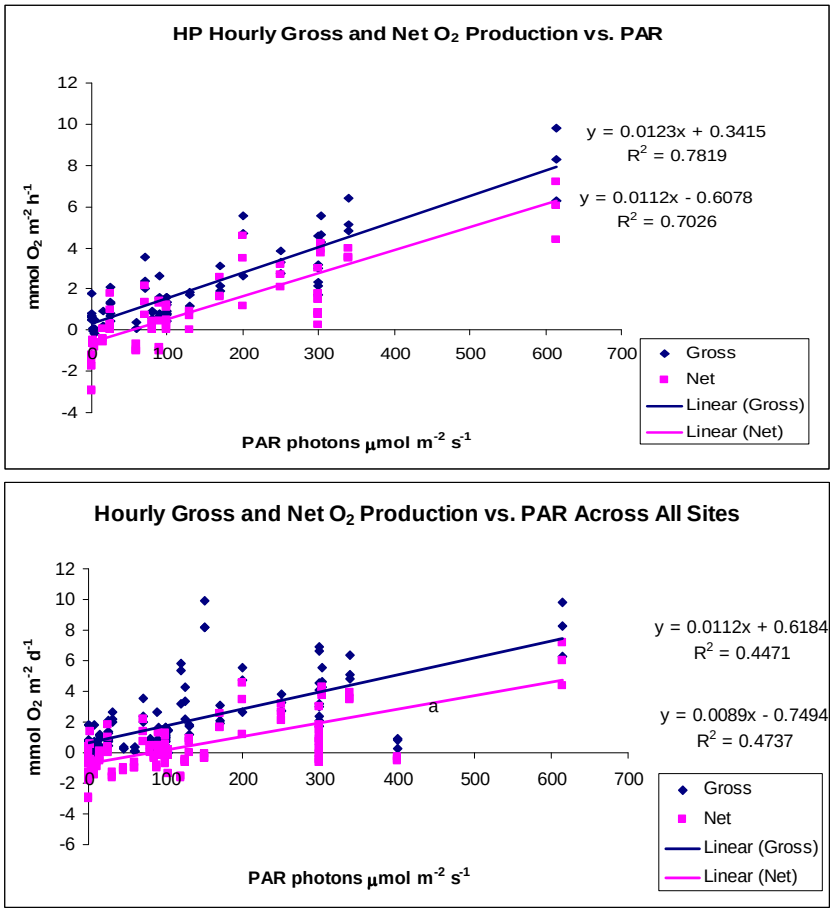

Figure 6. Correlation between PAR and net and gross O_2 production at the HP site and across all sites. Hourly net and gross relationships are significant P<0.05 in both HP and across all sites.

Table 3. R^2 values for net and gross O_2 production vs. PAR for the averages of all cores from each sampling sites. Only a few cores show significant correlation between PAR and O_2 production. N represents the number of depth stations per transect. In HP5, HP6, HP7 the 7meter site is included.

Sampling	Gross Hourly O_2 r^2	Sig. P<0.05	Net Hourly O_2 r^2	Sig. P<0.05	N
HP	0.98	no	0.96	no	3
HP2	0.99	yes	0.99	yes	3
HP3	0.89	no	0.95	no	3
HP4	0.99	yes	0.34	no	3
HP5	0.99	yes	0.98	yes	4
HP6	0.74	no	0.86	no	4
HP7	0.91	no	0.82	no	4
LTC	0.45	no	0.65	no	3

LTC2	0.01	no	0.33	no	3
LTC3	0.99	yes	0.91	no	3
FB	0.80	no	0.89	no	3
FB2	0.96	no	0.27	no	3
FB3	0.99	yes	0.15	no	3

Daily oxygen flux rates were also calculated. Daily gross O_2 (photosynthetic) production rates were obtained by the difference between hourly dark rates and light rates and multiplying by the hours of daylight on the sampling day. Daily respiration was obtained by multiplying the hourly dark rate by 24 hours. Net daily oxygen flux was calculated by multiplying the hourly dark rate by 24 hours to represent the background heterotrophic activity and then adding the daily gross production value to this daily respiration value.

Gross daily O_2 production rate = (light rate – dark rate, (μmol m^{-2} h^{-1}) * daylight hours

Daily respiration rate = dark rate (μmol m^{-2} h^{-1}) * 24 h

Net daily O_2 production rate = **Gross daily O_2 production rate - Daily respiration rate**

Daily net production was highly variable across seasons. The extremes occurred in the summer months (Figure 7), where the most positive and most negative rates were observed. The spring and winter months were characterized by rates closer to zero. The average daily net O_2 production for each season was -10.1 mmol m^{-2} d^{-1} for summer,

-10.1 mmol m^{-2} d^{-1} for spring, and -0.5 mmol m^{-2} d^{-1} for winter. The annual average was -8.4 mmol m^{-2} d^{-1}.

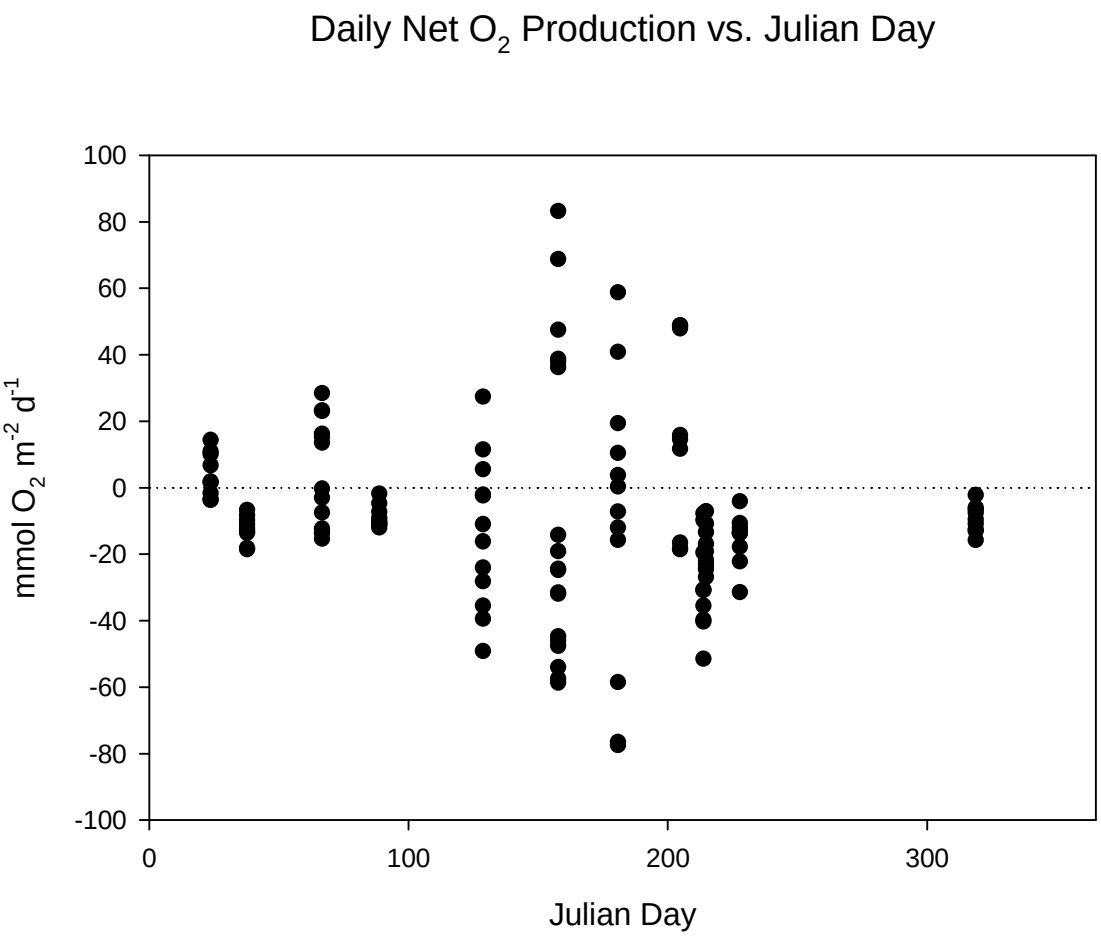

Figure 7. Daily net O_2 production vs. Julian day. As can be seen here, the widest range of net values are from the summer months for all sites. Positive rates suggest a net production of algal biomass, negative rates indicate net heterotrophy.

The HP sites had a daily net positive oxygen flux for most times at the shallow and mid-depth sample sites (Figure 8**)**. Both LTC and FB always showed net oxygen consumption. The average study-wide rates for HP shallow, mid-depth, deep, deepest for HP daily net O_2 flux rate were 23.5 mmol O_2 m^{-2} d^{-1}, 9.9 mmol O_2 m^{-2} d^{-1}, -14.4 mmol O_2 m^{-2} d^{-1}, and -42.2 mmol O_2 m^{-2} d^{-1} respectively. The LTC shallow, mid-depth and deep average daily net oxygen fluxes were -17.8 mmol O_2 m^{-2} d^{-1} , -26.2 mmol O_2 m^{-2} d^{-1} , -29.9 mmol O_2 m^{-2} d^{-1} respectively. For FB shallow mid-depth and deep daily net oxygen fluxes were -11.2 mmol O_2 m^{-2} d^{-1}, -18.6 mmol O_2 m^{-2} d^{-1}, and -24.4 mmol O_2 m^{-2} d^{-1} respectively. The highest observed daily net flux for all sites was 66.3 mmol O_2 m^{-2} d^{-1} at Horn Point in the shallow site and the study wide minimum net was at Horn Point at the deepest site with a rate of -71.1 mmol O_2 m^{-2} d^{-1}. Both FB and LTC experienced low net O_2 flux rates in summer 2006, with low rates at FB in August and LTC in June. Both sites had lower net O_2 fluxes in the spring of 2006.

At the HP site, daily gross O_2 production clearly scaled with depth, while at the FB and LTC sites there was no significant relationship between depth and gross production (Figure 8-9). The complete daily gross study-wide averages for each site were HP 25.3 mmol O_2 m^{-2} d^{-1}, LTC 11.1 mmol O_2 m^{-2} d^{-1} and FB 11.0 mmol O_2 m^{-2} d^{-1}. The highest positive value was the initial HP time point in June 2005 which had a rate of 119.9 mmol O_2 m^{-2} d^{-1}. The lowest value at the HP site was 0.4 mmol O_2 m^{-2} d^{-1} in June of 2006 at the deepest site.

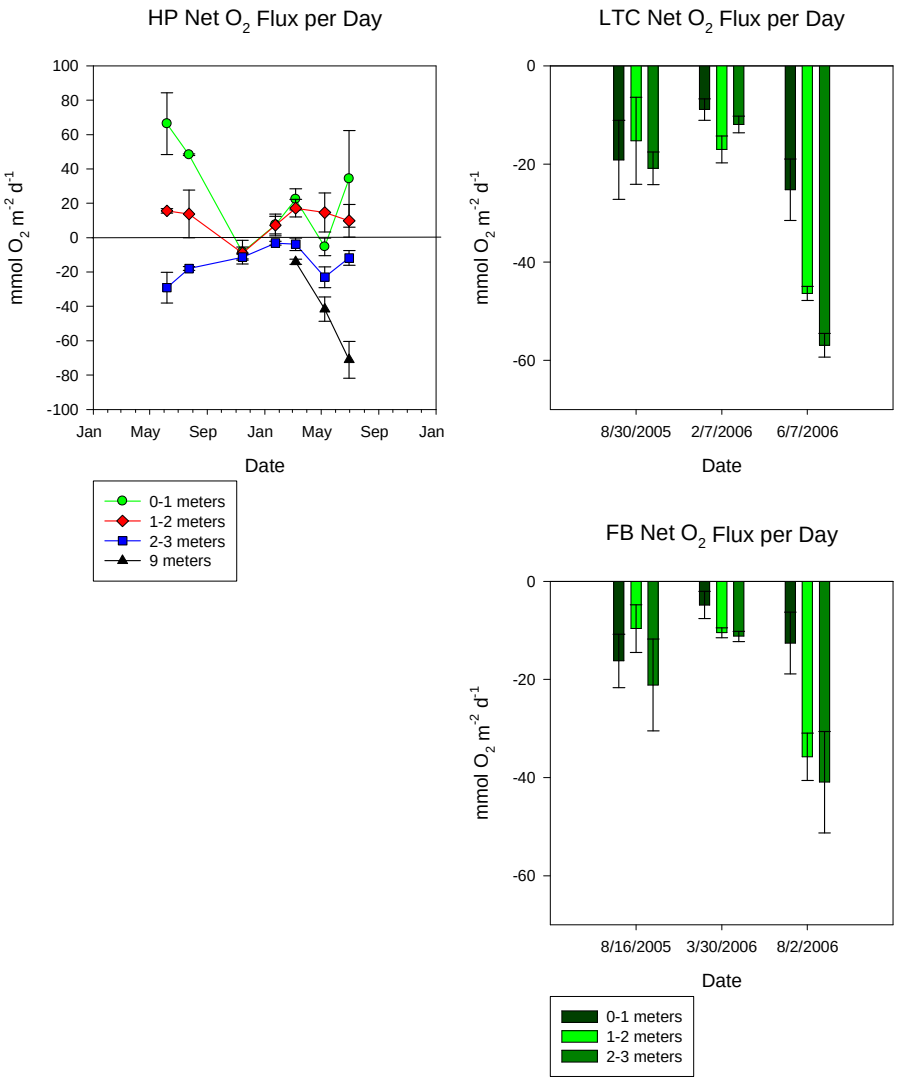

Figure 8. Net O_2 prod was calculated by multiplying the dark rate by 24 and the light rate by hours of sunlight per day and then summing the two values. Again, lines are to guide the eye not to suggest a contiguous trend.

Daily gross O_2 flux averages tended to be higher at HP in the late spring and summer than in the colder months of the year. The HP average for summer was 84.4 mmol O_2 m^{-2} d^{-1} and the average for winter and early spring was 23.9 mmol O_2 m^{-2} d^{-1}. At LTC, the highest average daily gross values were 33.5 mmol O_2 m^{-2} d^{-1} observed in June 2006 at the deep site; at FB the highest rate was 45.8 mmol O_2 m^{-2} d^{-1} on August 2006. The lowest O_2 flux rate for LTC was 4.8 mmol O_2 m^{-2} d^{-1} in Feb.

2006. The lowest rate at FB was 0.5 mmol O_2 m^{-2} d^{-1} observed in the shallow site in August 2005.

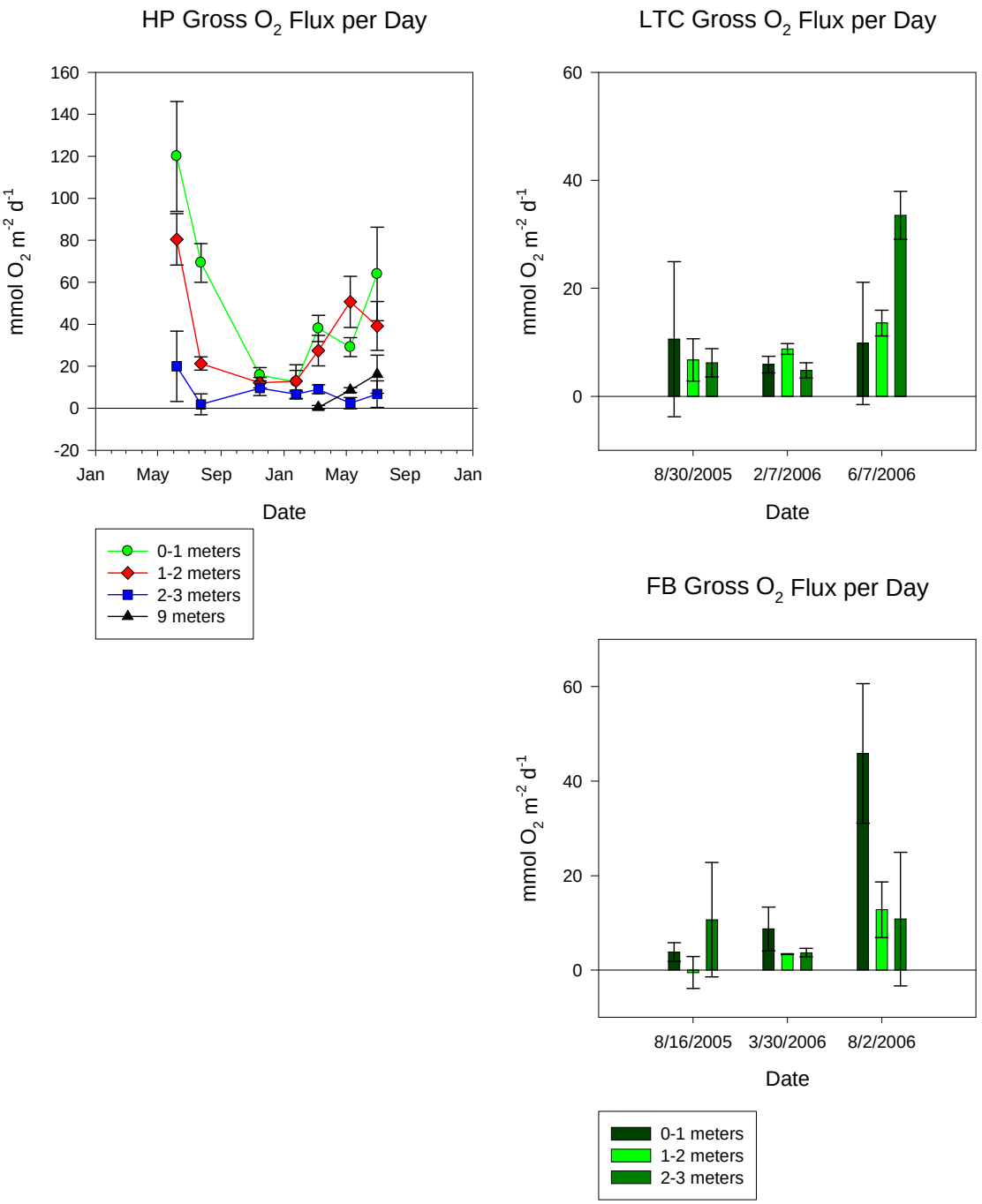

Figure 9. Gross O_2 flux for all sites. These are estimates of oxygen-based photosynthesis.

The relationship between depth and daily net/gross O_2 production was statistically significant, with a considerable amount of variability, especially at shallow depths ($P<0.05$) (Figures 10, 11). Though significant the r^2 values were low for daily gross oxygen flux and for net oxygen flux ($r^2 = 0.10$ and $r^2 = 0.12$). When the data is limited to just the HP site r^2 effect was higher with $r^2 = 0.44$ and $r^2 = 0.34$. The greater water transparency at the main HP sites resulted in higher O_2 production. LTC and FB had poorer transparency and changes in O_2 production were less dependent upon depth.

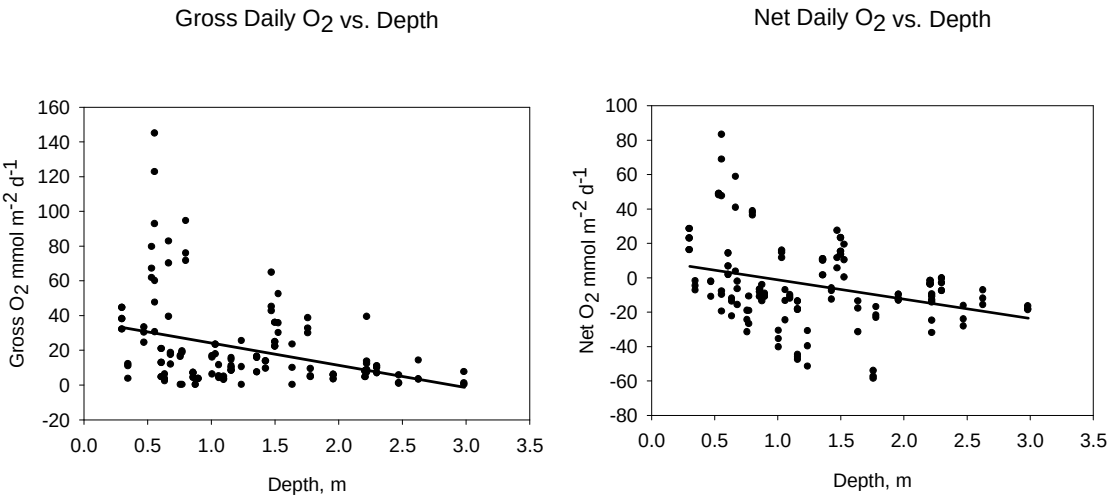

Figure 10. All gross and net oxygen fluxes plotted as a function of depth; data from all three locations are included. Relationships were significant ($p < .05$) Daily net $r^2 = 0.10$; daily gross $r^2 = 0.12$ Cores included all data except the 7 m deep Choptank cores.

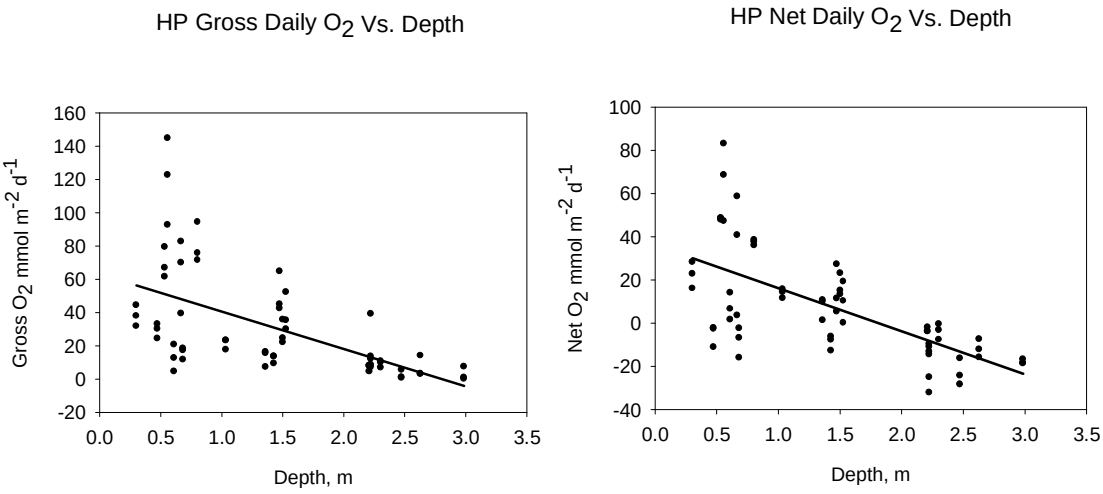

Figure 11. Plots of all HP gross and net oxygen fluxes as a function of depth.. Relationships are significant ($p < .05$, with an $r^2 = 0.44$ for daily gross and $r^2 = 0.34$ for daily net fluxes). Cores include all HP cores except the 9 meter deep cores which have no illumination.

At the HP site, Chl *a* values sometimes mirrored increases and decreases of daily gross and daily net O_2 production (i.e. photosynthesis) and sometimes photosynthesis appeared independent of chl *a*, as in the 0-1 meter sampling depth (Figures 12, 13). Chl *a* concentration tended to follow O_2 production best at 1-2 meters, and least at 0 to 1 meter. The inverse relationship between chl *a* and gross production at the initial HP sampling date is inconsistent with subsequent measurements but is possibly the result of the high irradiance in the outdoor incubation environment. Overall, chl *a* was significantly correlated with depth within the whole dataset though with a low r^2 (r^2=0.14) restricting the dataset to HP only created a stronger relationship. (r^2=0.40).

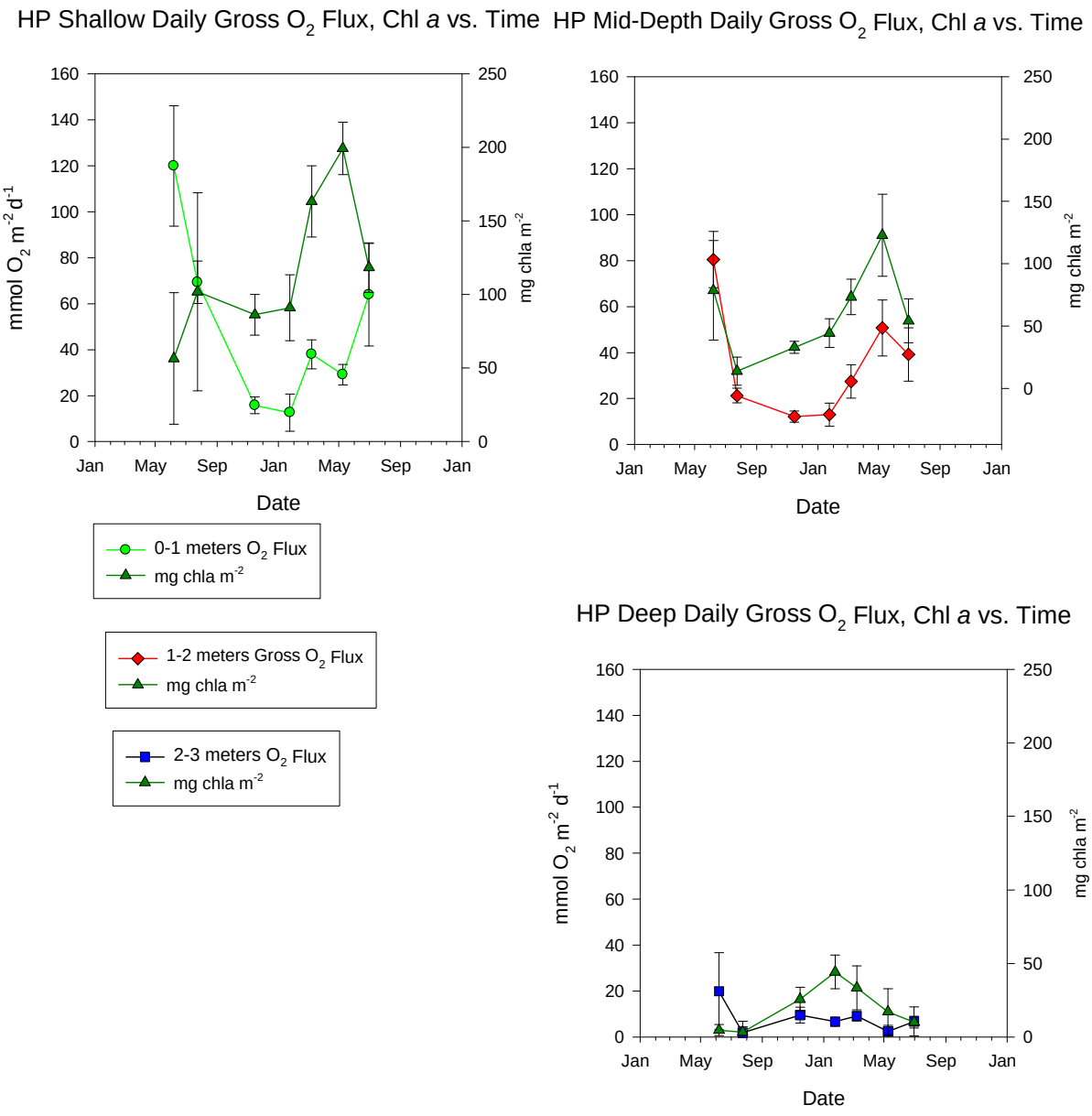

Figure 12. Daily gross O_2 production and chl *a* from sediment cores compared between months at HP.

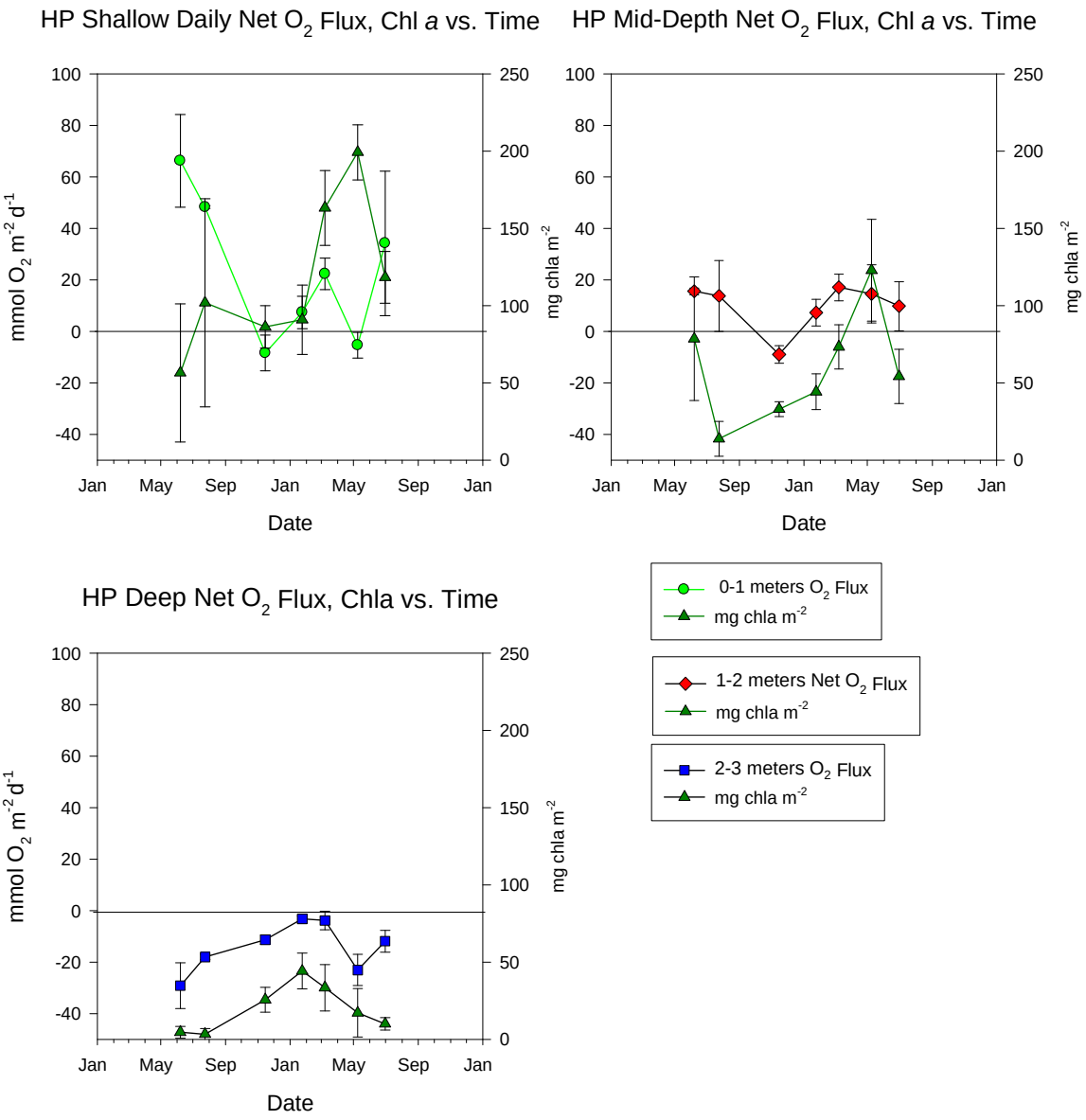

Figure 13. Daily net O_2 production and chl *a* from sediment cores between sampling dates at HP.

There was no significant relationship between chl *a* and gross or net O_2 production at FB or LTC as determined by regression analysis. Although O_2 production varied at a given site, chl *a* did not follow the trend of increase or decrease (Figures 14, 15).

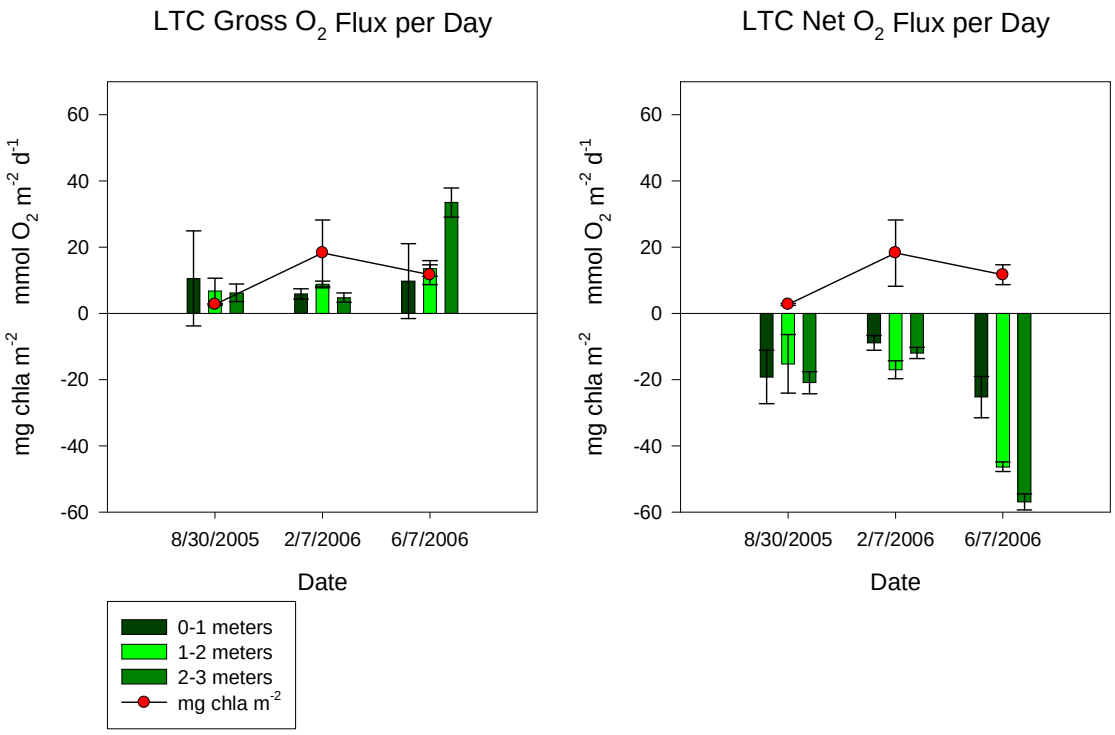

Figure 14. LTC gross and net O_2 production compared to average chl *a* taken from sediment cores.

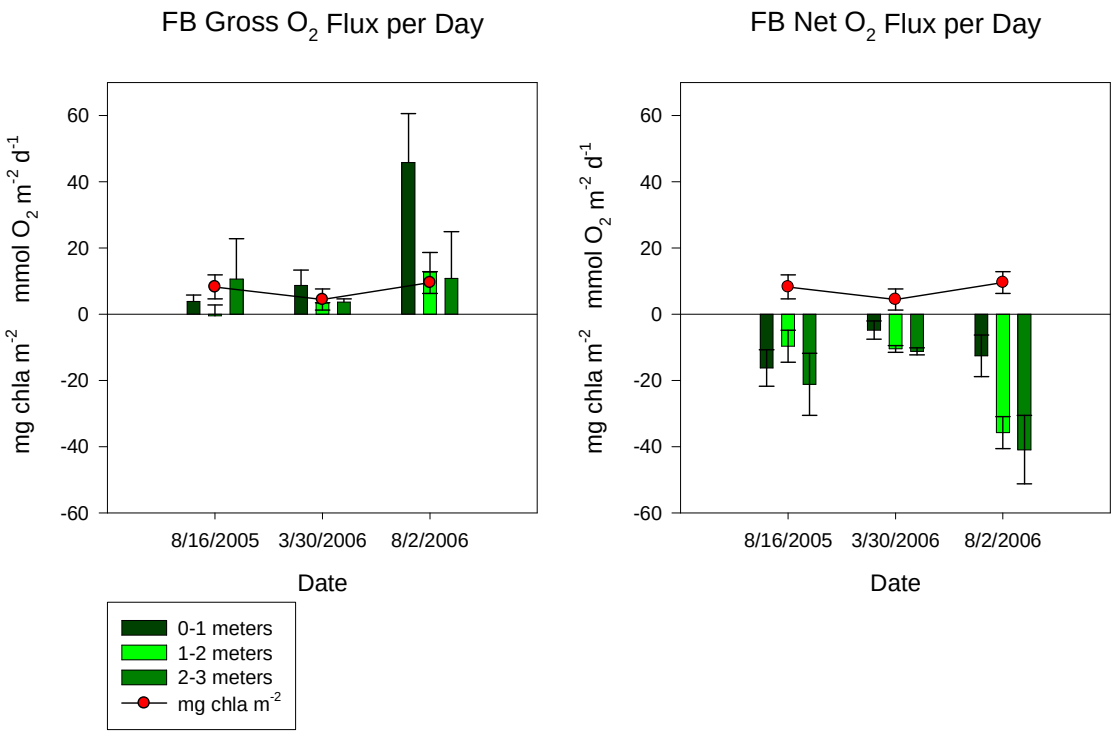

Figure 15. FB daily gross and daily net O_2 production compared to average chl *a* taken from sediment cores.

In this study there were significant seasonal relationships between chl *a* and net and gross O_2 production. The relationship was strongest during winter: r^2 =0.75 for daily gross production and r^2 =0.74 for daily net production (Figure 16**)**. The relationships between chl *a* and both net and gross oxygen fluxes was also highly significant in the summer (both had $p < 0.01$, $r^2 = 0.49$). During the spring there is a significant relationship between gross production and chl *a* content ($p < 0.01$; $r^2 =$ 0.55). There was no significant relationship between net production and chl *a* during spring. Stronger relationships between gross and net production in winter could be attributable to lower inputs of phytoplankton chl *a* and lower rates of sediment respiration. Less significant relationships in summer and spring are attributable to larger influxes of nutrients resulting in decreased light flux to the sediments. Lower

levels of irradiance have been shown to boost chl *a* concentrations in MPB, suggesting organisms maximize light utilization with lower illumination (MacIntyre et al. 1996).

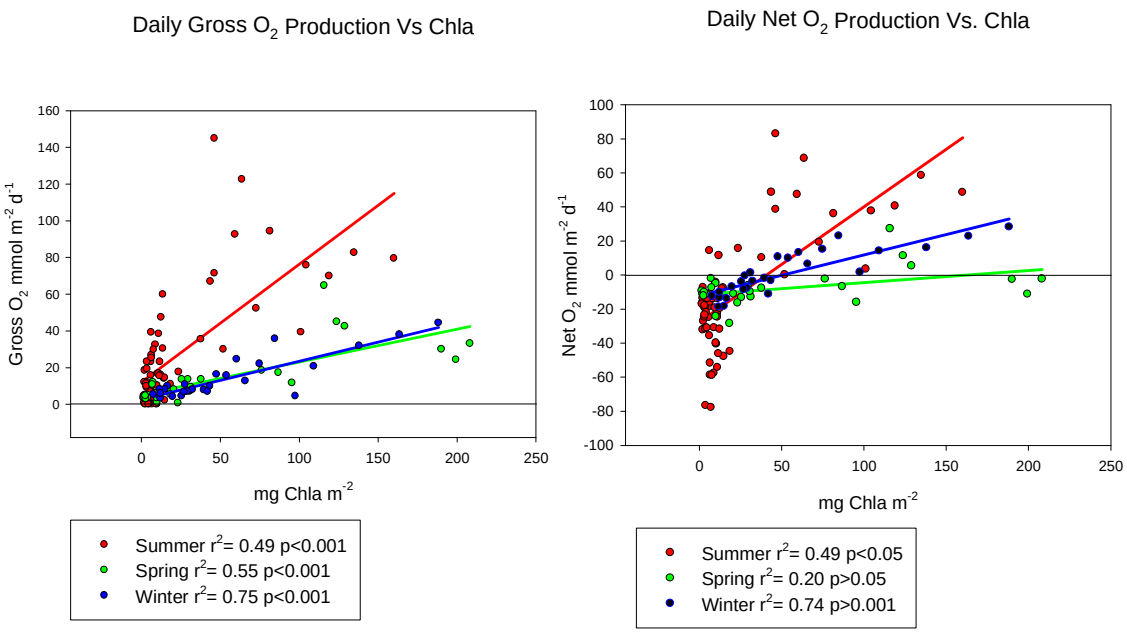

Figure 16. Daily gross and daily net O_2 production vs. chl *a*. This correlation was also done chl *a* with O_2 production rates normalized to biomass but the results did not produce a significant regression.

A series of multiple linear regressions was run to determine the most significant relationships between oxygen production and a series of environmental variables. These variables included daily gross production, net production and respiration O_2 flux, *k* (the PAR attenuation coefficient), chl *a*, nutrients, depth, percent sand, and irradiance. While, there was no significant effect of temperature, the core incubation data was split into three study-wide categories based on temperature to reduce variance; 0-10 C^o 10-20 C^o 20-30 C^o without regard to season.

Conveniently, this separated all the data into summer, spring and winter analysis groups; but there was insufficient data to create a separate fall analysis group. A combined annual analysis group was analyzed.

While light and percent sand together were highly significant factors in predicting O_2 production as shown in table 5, depth and percent sand were chosen as the two variables most useful for predicting O_2 production because data was readily available for ArcMap. The difference in r^2 between using depth and percent sand versus PAR and percent sand as predictors of benthic production was minimal. In addition during the winter, the relationship is slightly stronger when using depth and percent sand to predict net O_2 production.

Besides the strong correlations between depth, irradiance and O_2 production, there was a strong relationship during the winter between gross and net O_2 production and chl *a*. The winter also had a significant regression between gross production and the attenuation coefficient, indicating the importance of water quality in predicting rates of photosynthesis.

Percent sand, by itself, did not have a significant relationship with production except during the winter months between net and respiration. However, when combined with depth or light, percent sand improved the r^2 value of the resultant multiple linear regression.

Table 5. Data set wide results of linear regression r-squared values of daily respiration, daily gross O_2 production, and daily net O_2 prod. Multiple linear regression of net vs. sand and depth produced the highest r-squared value. *Indicates all variabiles were significant in the regression. The N for yearly analysis was 126 cores. Summer N was 67 cores. Spring N was 31 and winter N was 31.

Season	All	PAR+Sand	*k*	Chla	PAR	Depth	Sand	Dep,+Sand.
Yearly	Resp.	0.131	0.008	0.008	0.000507	0.0637	0.0866	0.0872
	Gross	0.381*	0.0207	0.229	0.311*	0.132	0.103	0.269
	Net	0.445*	0.00457	0.292	0.267	0.193	0.294	0.454*
Summer	Resp.	0.176	0.155	0.00184	0.00392	0.152	0.103	0.103
	Gross	0.761*	0.185	0.499*	0.786*	0.0636	0.179	0.409*
	Net	0.809*	0.0164	0.487*	0.611*	0.255	0.387	0.595*
Winter	Resp.	0.586	0.0439	0.0521	0.115	0.00347	0.558*	0.559
	Gross	0.526*	0.559*	0.753*	0.190	0.237	0.236	0.489*
	Net	0.747*	0.310*	0.736*	0.0519	0.201	0.597*	0.774*
Spring	Resp.	0.504	0.261	0.640*	0.0202	0.481	0.191	0.203
	Gross	0.327	0.000184	0.556*	0.259	0.0280	0.0804	0.152
	Net	0.104	0.166	0.200	0.167	0.555	0.00775	0.105

The following equations were used to predict O_2 production depending on season and significance.

Summer Net = -11059.6 - (22476.8 * depth) + (549.0 * sand) r^2= 0.60

Summer Gross = 35595.12 - (22951.0 * depth) + (374.5 * sand) r^2= 0.41

Yearly Net = -11261.6 - (15456.3 * depth) + (389.98 * sand) r^2= 0.45

Yearly Gross = 26879.1 - (16146.6 * depth) + (243.4 * sand) r^2= 0.27

Winter Net= -7047.6 - (8282.7 *depth) + (277.9 * sand) r^2= 0.77

Winter Gross= 15132.3 - (8556.5 * depth) + (151.5 * sand) r^2= 0.49

Spring net production did not have a significant correlation; however this equation was used speculatively to examine the spatial relationships during spring:

Spring Net = -5136.180 - (5149.388 * depth) + (48.232 * sand) r^2= 0.105

These equations were used as inputs into the attribute table of ArcMap 9.2 and used in combination with the spatial bathymetry and percent sand shapefiles to predict daily net and gross O_2 production in the Mid-Bay region. The core-derived sediment grain size data and sample location bathymetry were used as input into these equations and plotted against the measured data as a measure of the quality of the benthic extrapolations (Figure 17).

The models of gross and net production were significantly related to the observational data (Figure 17), with considerable scatter ($P<0.5$). Winter daily net was the most highly correlated with an r^2 of 0.68, followed by summer with an r^2 of 0.46. The annual net correlation had an r^2 of 0.43, and the summer daily gross correlation had the least amount of correlation with an r^2 of 0.34. Annual daily gross and spring daily net did not have significant correlations with the measured data.

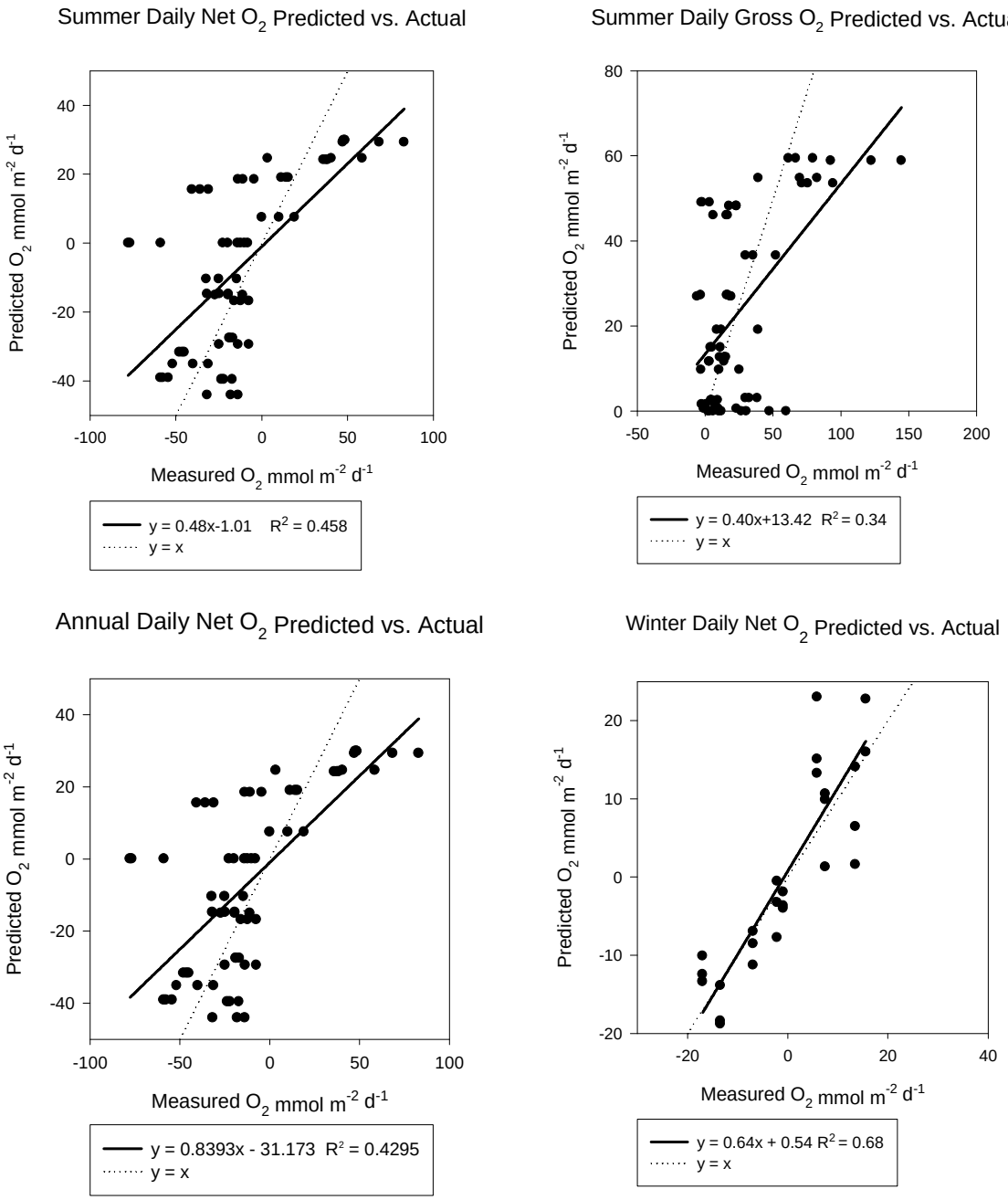

Figure 17. Predicted vs. measured daily O_2 production rates. Measured values are from the core flux measurements; predicted values are from the ArcMap output. Negative values in the gross figure demonstrate the weakness of the model. Y=x represents a perfect correlation between measured and predicted.

Discussion

Using the data relationships developed in the previous section, spatial predictions of the distribution of net oxygen flux and photosynthesis were made using ArcMap 9.2 (Figures 18-21). Areas of highest predicted oxygen flux (i.e. positive values or values that were *less negative*) were located adjacent to shore and rates decreased gradually away from the shore (Table 6). Note that no predictions were made below 3 meters in depth. Those predictions which appear to extend beyond 3 meters are an artifact of the extrapolation. The remnants of Sharps Island in the mouth of the Choptank River showed a strong positive oxygen flux during the summer and winter. The ArcMap model produced results which varied greatly by season. The winter map had the largest area of net autrophic sediments, consistent with more transparency and lower rates of respiration. In the summer (Figure 19) there is higher production near the shore but net heterotrophic sediments were found in shallower areas than in the winter. Greater light attenuation and higher sediment respiration during the winter are the proximal causes. The spring map (Figure 20) is based on non-significant correlations, but suggests that spring blooms strongly affect MPB production. Spring phytoplankton blooms generate high attenuation and result in lower irradiances to the benthic light environment (Kemp et al 2005). This would result in the decreased spring net benthic productivity.

It is common for MPB sediments to be characterized by net heterotrophy (Fear et al. 2004; MacIntyre et al. 1996). Summer predictions showed shallow areas of intensive net positive O_2 flux with sediment O_2 demand increasing rapidly down

the depth gradient. Consequently, summer conditions had both the highest measured rates of O_2 production and the highest rates of sediment O_2 demand (Table 7). Higher temperatures and increased PAR to the water surface lead to higher rates of shallow water photosynthesis but lower net rates in the deeper water depths due to higher light attenuation.

Low temperatures and relatively low turbidity in the winter resulted in a greater area of net autotrophy (i.e. to greater depths) but with lower photosynthetic rates (Figure 21). MPB has been demonstrated to be both a short-term sink and a barrier for N and P release in shallow water sediments (Sundback et al. 2000; Engelsen et al. 2008). This net photoautotrophy can have an affect in sequestering nutrients in shallow water CB sediments. Decreased nutrient fluxes from shallow sediments are expected during the winter and summer seasons, and increased nutrient fluxes are expected during the spring. A decrease in shallow water nutrient flux along with a positive O_2 flux from the sediment may reduce the potential effects of increased shallow water respiration.

Table 6. Total is listed as net kg O_2 d^{-1} for all bathymetry 0 to 3 meters in depth which is an area of $2.58x10^8$ m^2. The average is listed in mg O_2 m^{-2} d^{-1} average represents area weighted mean.

Season	Total O_2	Average Net O_2	S.E.
Annual	$-3.36x10^5$	-1303	336
Summer	$3.18x10^4$	123	962
Winter	$3.92x10^4$	152	413
Spring	$-6.62x10^4$	-257	123

Table 7. Values listed as net O_2 mg m^{-2} d^{-1} for each depth interval across all seasons which have a significant relationship with depth, percent sand and productivity.

Depth,m	Winter mg m^{-2} d^{-2}	S.E.	Summer mg m^{-2} d^{-2}	S.E.	Spring mg m^{-2} d^{-2}	S.E.	Annual mg m^{-2} d^{-2}	S.E.

0	-22	226	399	437	-90	39	-174	310
1	-131	219	-277	424	-258	38	-700	301
2	-322	229	-1112	444	-440	39	-1112	315
3	-453	229	-1831	444	-611	39	-1607	315

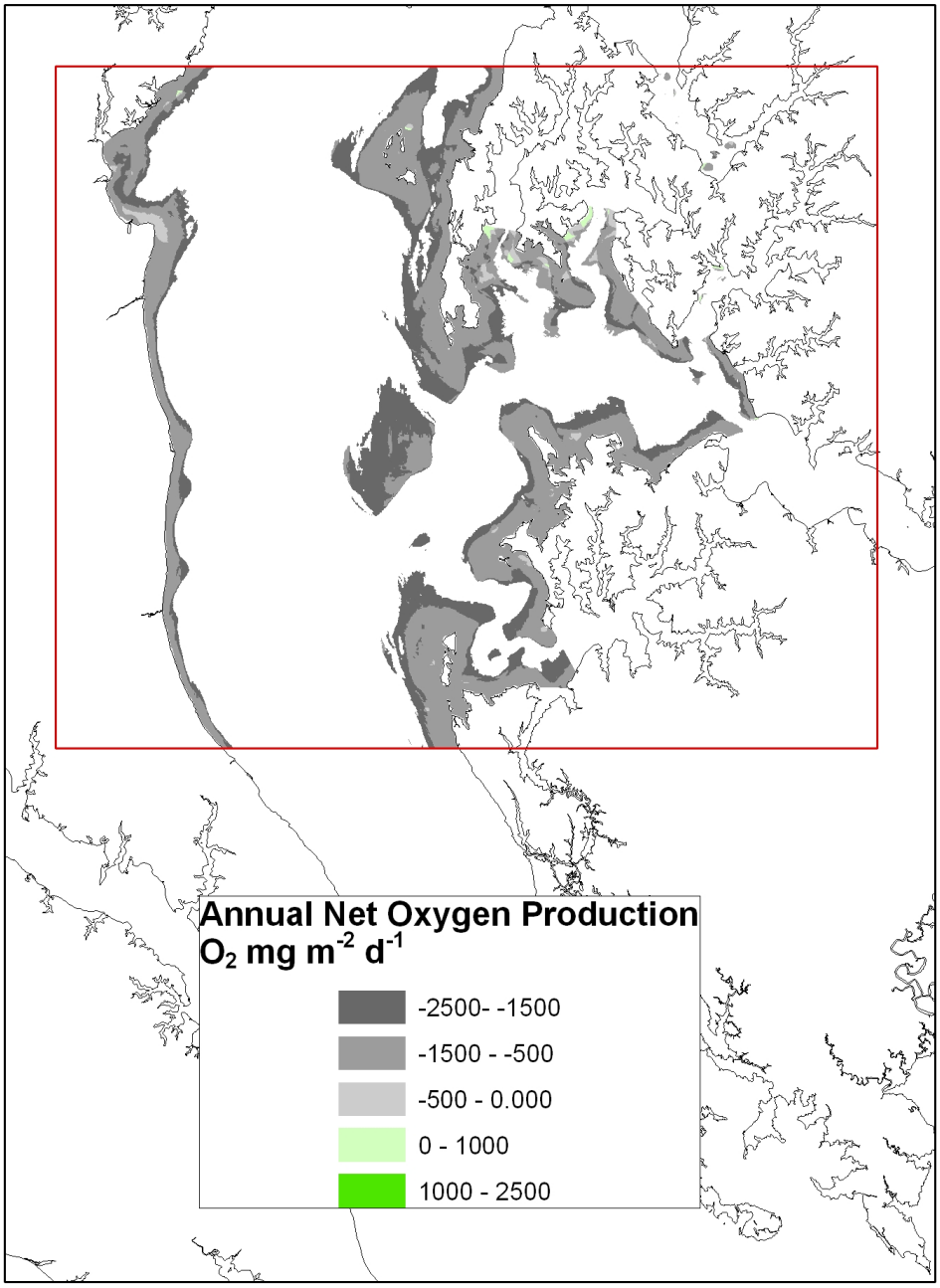

Figure 18. Annual predicted benthic daily net O_2 production.

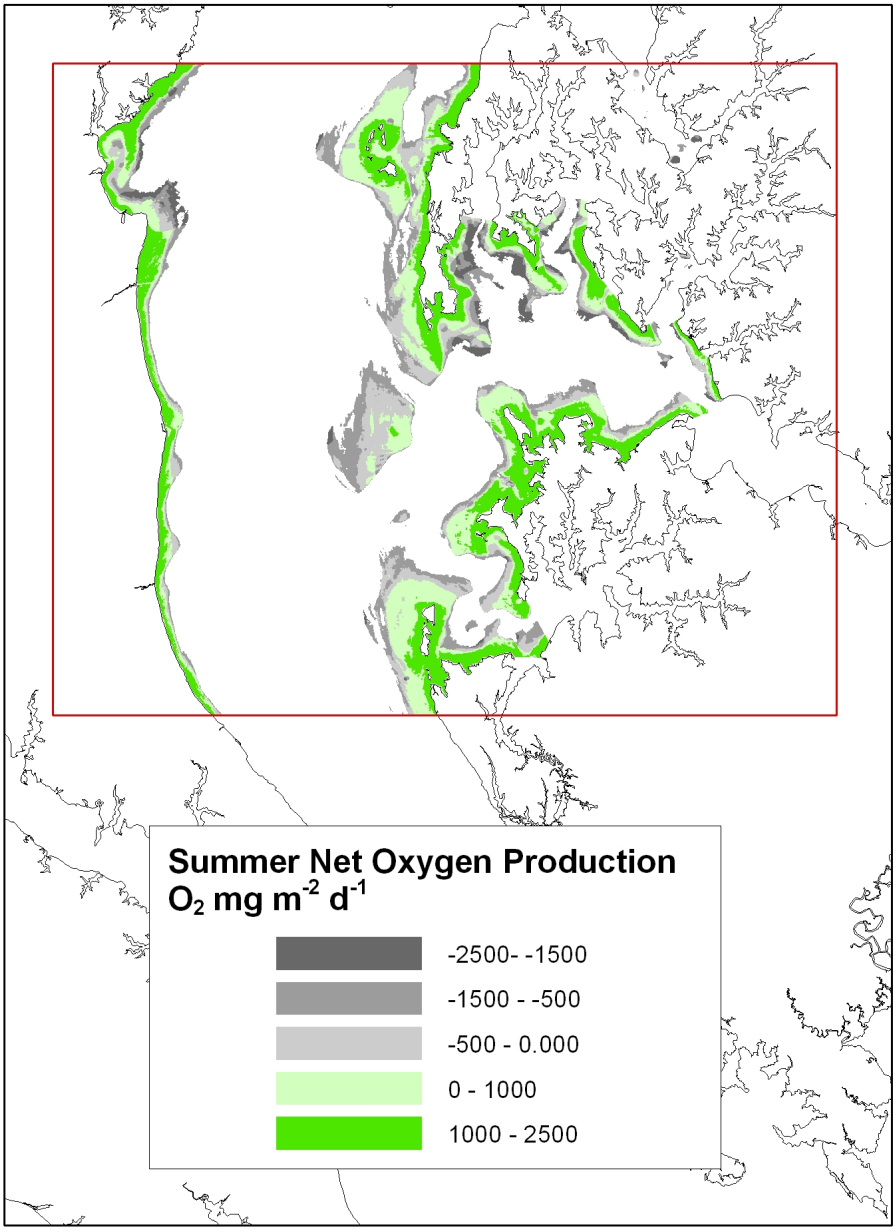

Figure 19. Summer benthic daily net O_2 production

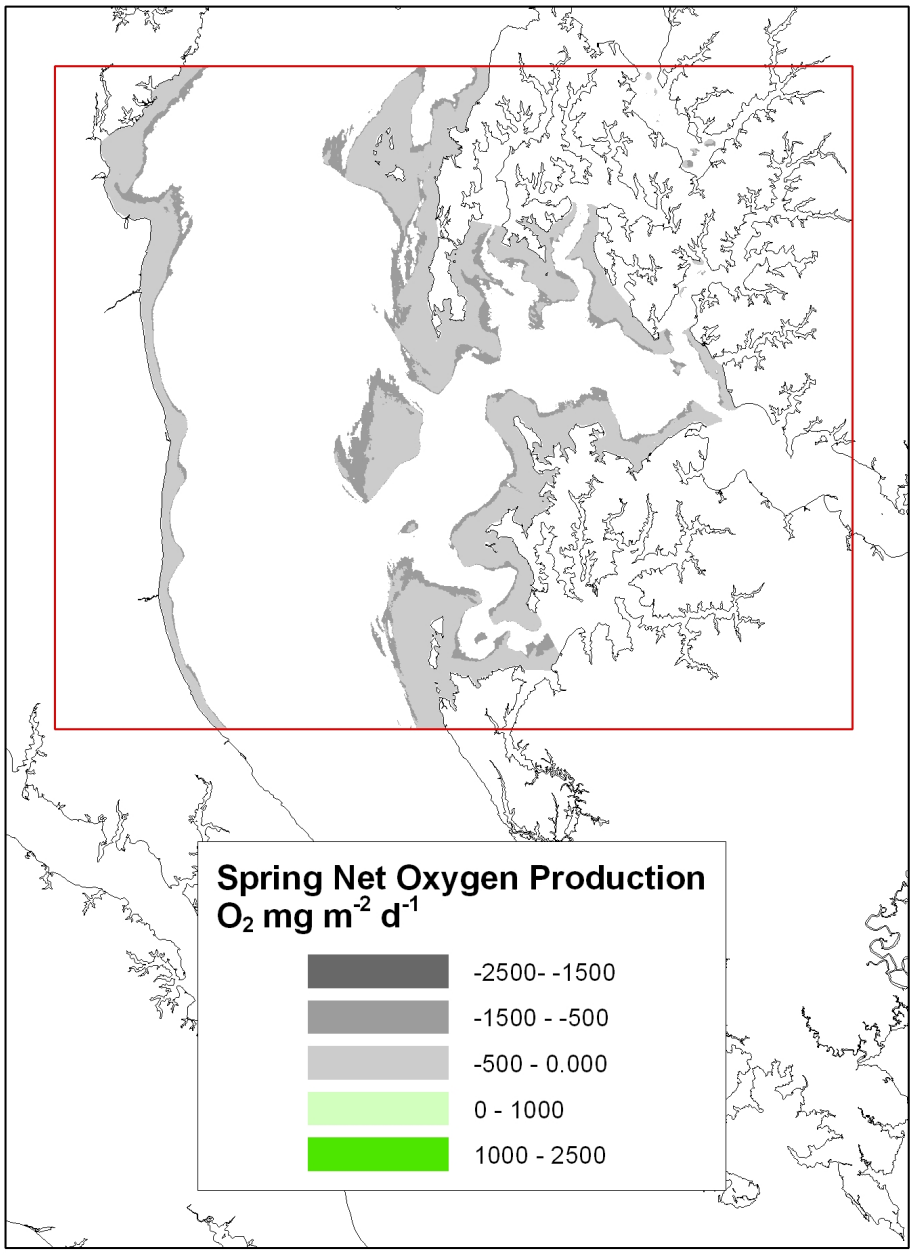

Figure 20. Spring benthic daily net O_2 production.

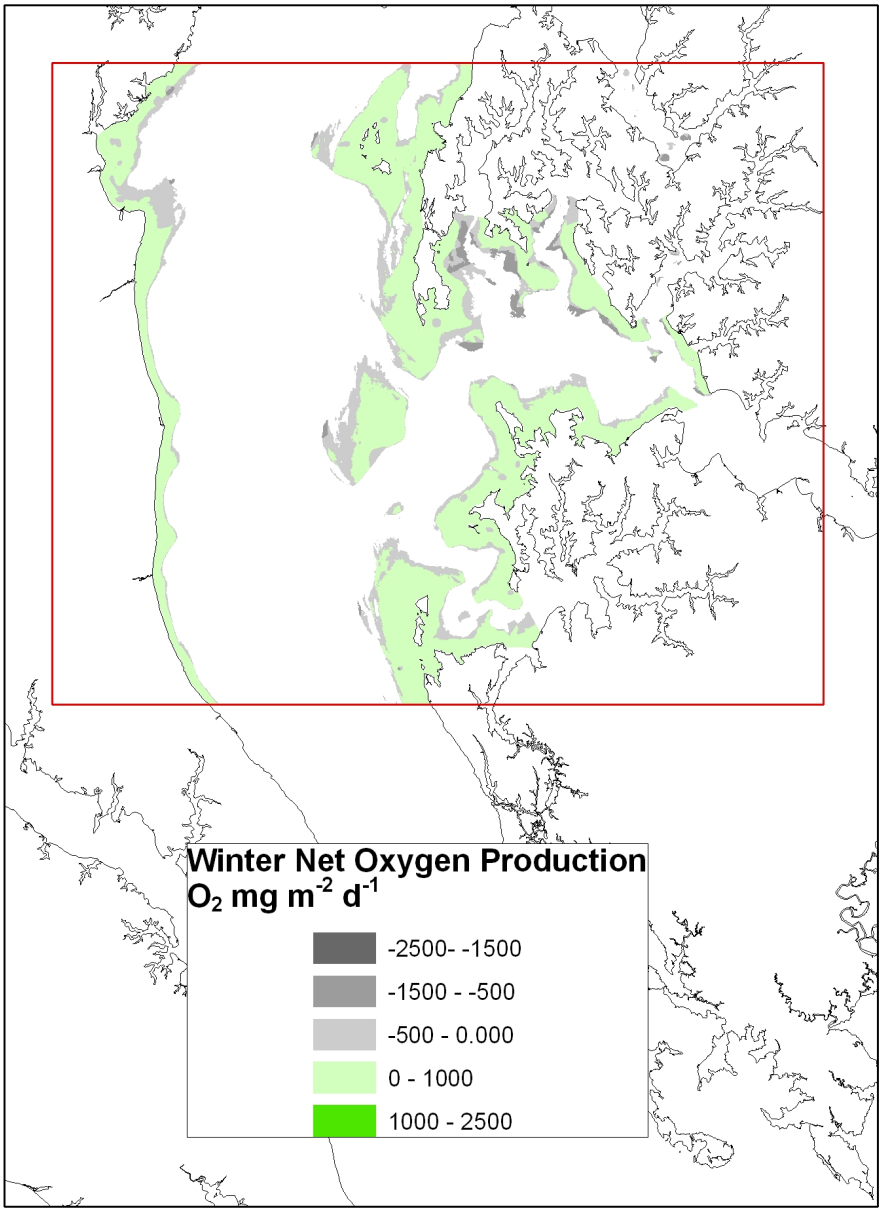

Figure 21. Winter benthic daily net O_2 production

The seasonal and annual predicted gross O_2 rates in this study for production were lower than Reay et al.'s (1995) rates from the southern Chesapeake Bay (Table 6). Reay et al. (1995) presented rates which represent a seasonal integration of primary production in carbon units per meter squared. In order to convert the oxygen flux units to units comparable to Reay et al. (1995), the assumption was made that the benthic ratio for carbon atoms to oxygen atoms in primary production was 1:1 and daily O_2 was converted to C. Values were then multiplied by the number days of each season. Reay et al. (1995) reported annual primary production of 515 g C m^{-2}, considerably higher than our annual value of 66 g C m^{-2}. Summer primary production for Reay et al. (1995) was 271 g C m^{-2} compared to 30 g C m^{-2} in this study. Spring and winter were also much higher than respective rates in this study. The difference is attributed to the inclusion in this study of low productivity in the FB and LTC environments. The biomass normalized photosynthetic rate mg (mg C mg $chla^{-1}$ h^{-1}) falls within the range of other MPB study sites (Table 7).

Daily gross and daily net O_2 flux rates were similar in shallow water to those measured in North Carolina's Nuese River Estuary (Fear et al. 2004). The average of all shallow light phase O_2 fluxes was 1.1 mmol m^{-2} h^{-1} compared to -0.6 mmol m^{-2} h^{-1} in the shallow light treatment in Fear et al. Deep dark O_2 fluxes in this study were -1.2 mmol m^{-2} h^{-1} compared to -1.4 mmol m^{-2} h^{-1} in the Neuse River.

Table 6 Values were converted to carbon units using a 1 to 1 conversion ratio to compare to Reay et al. (1995) Values represent gross primary production.

Season	This Study g C m^{-2}	Reay et al. (1995) g C m^{-2}
Spring	16.4	107.36
Winter	15.1	47.8
Summer	37.4	270.1
Annual	66.5	515.1

Table 7. Values from each depth represent daily gross values converted to Carbon mass on 1 to 1 ratio and divided by 24 for the hours in a day.

Reference	Location	mg C mg chl a^{-1} h^{-1}	Error
This study	0-1 meters	0.53	0.65
This study	1-2 meters	0.47	0.38
This study	2-3 meters	0.69	0.69
Rasmussen et al. (1983)	Danish Sea	0.16-0.57	-
Rivkin et al (1987)	Antarctic	0.53-0.60	-
MacIntyre et al. (1995)	San Antionio Bay, TX	~1-12	-
Meyercordt et al. (1999)	Baltic Sea	0.5-8.80	-
Miles et al. (2000)	SWE, ITA, POR	0.26-0.52	-

The significant relationship between percent sand and O_2 production can be attributed to the land use of the nearby sampling locations. Both FB and LTC have a high proximity to mesohaline fluvial marsh water inputs. These marshes in many cases are adjacent to agriculture and have resultant high sediment flows. This terrestrial sediment flow impacts both water quality which limited photosynthetic rates and MPB abundance and deposits fine grain sediments on the water-sediment interface. In contrast, the HP site is further downstream from fluvial inputs and has considerably more fetch. Being further from the source of these sediment inputs may

result in better water quality conditions compared to the sites adjacent to inputs and less sediment deposition. The increased flow from wave action would also result in the predominance of heavier grained sediment.

Another explanation for this relationship could be that larger grain sediments allow for less light attenuation past the water-sediment interface and this could result in higher rates of photosynthesis. It has been observed that larger grain sediment allows deeper light penetration and less light attenuation past the sediment-water interface (Ichimi et al. 2008).

The significant relationship between depth and O_2 production is driven by the significant relationship between PAR and O_2 production, as depth is a proxy for irradiance in this extrapolation. In this experiment, PAR was a significant predictor of O_2 production during the summer and during the annual gross regression. The strong relationship in the summer can be attributed to the seasonal net O_2 production in the 0-1 meter sampling point and perhaps the more negative O_2 production in the 2-3meter sampling depth (Table 8). Summer is typically characterized by higher temperatures and higher irradiances which provide MPB with their most limiting resource, irradiance. At deeper depths and greater water column volume, increased summer phytoplankton cause higher attenuation. A possible reason for the significant annual gross relationship with PAR is that gross production is a direct measure of total photosynthetic activity and thus is more tightly driven by available irradiance.

A recent analysis suggests that MPB contributes less than 10% of total bay productivity (Kemp et al. 1999) with the remaining being shared between SAV and pelagic phytoplankton. From the 1960s to the 1980s, submerged aquatic vegetation

(SAV) in a Susquehanna seagrass bed was observed to drop from an estimated coverage of 100% to lower than 10% (Kemp at al. 2005). This decrease in SAV meant that a larger fraction of Bay primary productivity was being produced through MPB. This study estimated the proportion of MPB contribution to total primary production without including SAV in the estimate as it appears that as water quality declines SAV will become a less significant contribution to O_2 (Kemp et al. 2004).

Average benthic photosynthetic rates were compared with pelagic production rates from Harding et al. (2002). The Harding et al. (2002) data were presented as seasonal rates calculated from pelagic ^{14}C experimenets. In order to compare the predicted benthic values to the Harding et al. data, the pelagic rates were converted from carbon primary production rates to O_2 rates. These rates were converted to O_2 rates by multiplying the molar equivalent of net pelagic values by 1.48 and the gross by 1.38 (Harding et al. 2002) and then converting back to O_2. This ratio is different than the 1:1 ratio used to compare to the Reay et al. (1995) data because it was necessary here to produce units using Harding et al.'s photosynthetic quotient.

In order to calculate the rates of pelagic production at each depth, these pelagic rates were multiplied by the area of each meter depth interval. At each depth interval the pelagic production was subtracted away in a proportion equal to the decrease in size of the water column. Although there is a non-linear relationship between pelagic primary production and depth, pelagic primary production over depth was treated as a linear relationship for simplicity's sake. Thus at a depth of 1 meter, the pelagic production of 1 meter was compared to the predicted gross benthic production of 1 meter. This calculation was done to account for the shrinking water

column as the proximity to the shore decreases. The ratio of benthic to pelagic production at each depth was then used as an attribute in ArcMap (Figures 22-23). It is recognized that current models of pelagic production suggest that photosynthesis decreases away from the surface in a logarithmic fashion, however we have used a linear curve in the interests of simplicity.

In order to calculate a proportion of production representing the entirety of the Mid-bay region, we multiplied the area of the Mid-bay with a depth deeper than 3 meters by the seasonal pelagic production values. We then summed this open-water pelagic production value with the individual depth specific pelagic production values from 0-3 meters and created a proportion of total benthic gross production to gross pelagic production.

This analysis is seasonally limited by a lack of significant benthic relationships during spring and fall. Thus, only comparisons using annual values and summer values are possible. The benthic pelagic gross production ratios for summer were twice as high as those for the annual prediction at depths less than 3 meters (Table 8). This suggests a larger contribution of MPB to primary production during the summer months.

Table 8. Benthic gross production over pelagic production, pelagic production was adjusted for the depth. No units are present because values are represented in ratios.

Depth	Annual	Summer
	Benthic:Pelagic Production Ratio	
0-3	2.51	4.69
0	6.53	12.1
1	1.39	2.68
2	0.4	0.72
3	0	0

This seasonal shift may have significance for the interaction of shallow water food webs in the Chesapeake. MPB is a primary food source for benthic invertebrate herbivores which in turn support a predatory community of fish and shellfish (Galvan et al. 2008). This may be a driver of seasonal shifts in food web dynamics as the relative availability of this MPB food source changes affecting populations of shellfish and demersal fish (Vedel et al. 1998). In contrast, as the relative importance of MPB to pelagic production shifts seasonally populations of herbivores may shift to pelagic consumers.

By adding the estimated values of gross pelagic and gross MPB production and then fractioning the MPB values for the area in which this estimation was performed (Figure 1), I calculated the proportion of primary production contributed by MPB to be approximately 12%. Similar production estimates have been made for the Seta Inland Sea Japan (Sarker et al. 2009)

Large site to site differences in MPB biomass and O_2 production were observed, with the highest positive O_2 flux rates observed in shallow water sediments of the mainstem Choptank River. The two more turbid sites (LTC and FB) were always net heterotrophic. Increased nutrient loads have been associated with locations and seasons characterized by high nutrient input and sediment load (Gallegos & Jordan 2002). Water quality has been the primary driver behind benthic primary production in CB, fluctuating with season and precipitation (Kemp et al. 2004). The HP site, which experienced higher net O_2 flux and chl *a* concentrations, was further downstream of fluvial inputs and had consistently lower attenuation

coefficients, facilitating an improved light environment over FB and LTC. The proximity to nutrient inputs and fluvial suspended material from local creeks and rivers likely disrupted the expected relationship between chl *a* concentration and O_2 production at FB and LTC. In addition, chl *a* from these sites may reflect non-MPB sources such as deposition from the water column of phytoplankton. Thus, the level of measured benthic primary production was higher and this could potentially boost the abundance of MPB-dependent higher trophic organisms. MPB production and abundance have been shown to support meiofauna populations (Pinkney et al. 2003, Sullivan and Moncreif 1990), but no evidence exists to suggest MPB is a controlling factor for meiofauna. Nevertheless, the existence of thriving MPB population could provide nutrition for organisms of higher trophic levels. It would be an interesting mesocosm experimental study to determine the extent of meiofaunal ecological dependency on MPB.

As mentioned above, depth and sediment grain size were used to predict net and gross oxygen production in this study. While depth is directly related to available light, the significant sediment relationship may be a result of the sediment input to the LTC and FB system. The high sediment loads from fine grained sediment particles may result in lower water quality and smaller grain size. This suggests a possible correlation between sandy sediments and abundance of associated meiofauna in the Chesapeake Bay as MPB has been observed to be a primary food source for snails, nematodes, and crustaceans (Pinckney et al. 2003, Montagna 1984, Moncrief and Sullivan 2001). It has previously been observed in Rizzo et al. 1996's benthic trophic system index (BTSI) that sandy sediments demonstrate a higher net O_2 flux in

Chesapeake Bay sediments and North Carolina sediments. However, sandy sediments may be limited in organic matter in comparison to smaller grained sediments, but smaller grained sediments in the Chesapeake Bay may be associated with higher nutrient inputs.

Overall, net benthic microalgal O_2 production rates were highest in the summer and lowest in the spring. Light attenuation was negatively correlated with O_2 production during the winter months and the attenuation constant measurements were lower during the winter sampling dates as well (Table 5). Increased nutrient loads during the spring and early summer are likely the cause of the spring decrease in water quality (Hay et al. 2004). This seasonal decrease in O_2 production results in changes in sediment redox boundries and may restrict denitrification during periods of low water quality (Sundback et al. 1991; An and Joye 2001; Risgaard-Petersen 2003). In addition, lowered MPB production and abundance may affect nutrient efflux from the sediment-water interface as biomass is reduced in the spring. Though some MPB populations may be nutrient limited, (de Jonge 1999), MPB populations do not respond to spring nutrient influxes suggests that this perhaps is not the case in the Chesapeake Bay.

Despite the shallow nature of the Chesapeake, benthic microalgal production is much smaller than pelagic production and contributes ~12% of total primary production in those locations without SAV coverage. In the 0 to 3 m range, benthic microalgal production is higher than that produced by pelagic organisms. This is amplified during the summer months. Increased water clarity in the Chesapeake Bay would result in an extended compensation depth and an increase in benthic O_2

production (Fear et al 2004). This would extend the benefits of MPB (increased oxygenation of sediment, nutrient retention, food source) to deeper depths of the Chesapeake Bay. However, a slight improvement in water quality has, in recent years, led to a gradual repopulation of SAV in some areas of the Bay (Kemp et al. 2004). It is probable that as the Chesapeake Bay's eutrophic state is improved an increase in available light will encourage more macrophytic production as opposed to MPB.

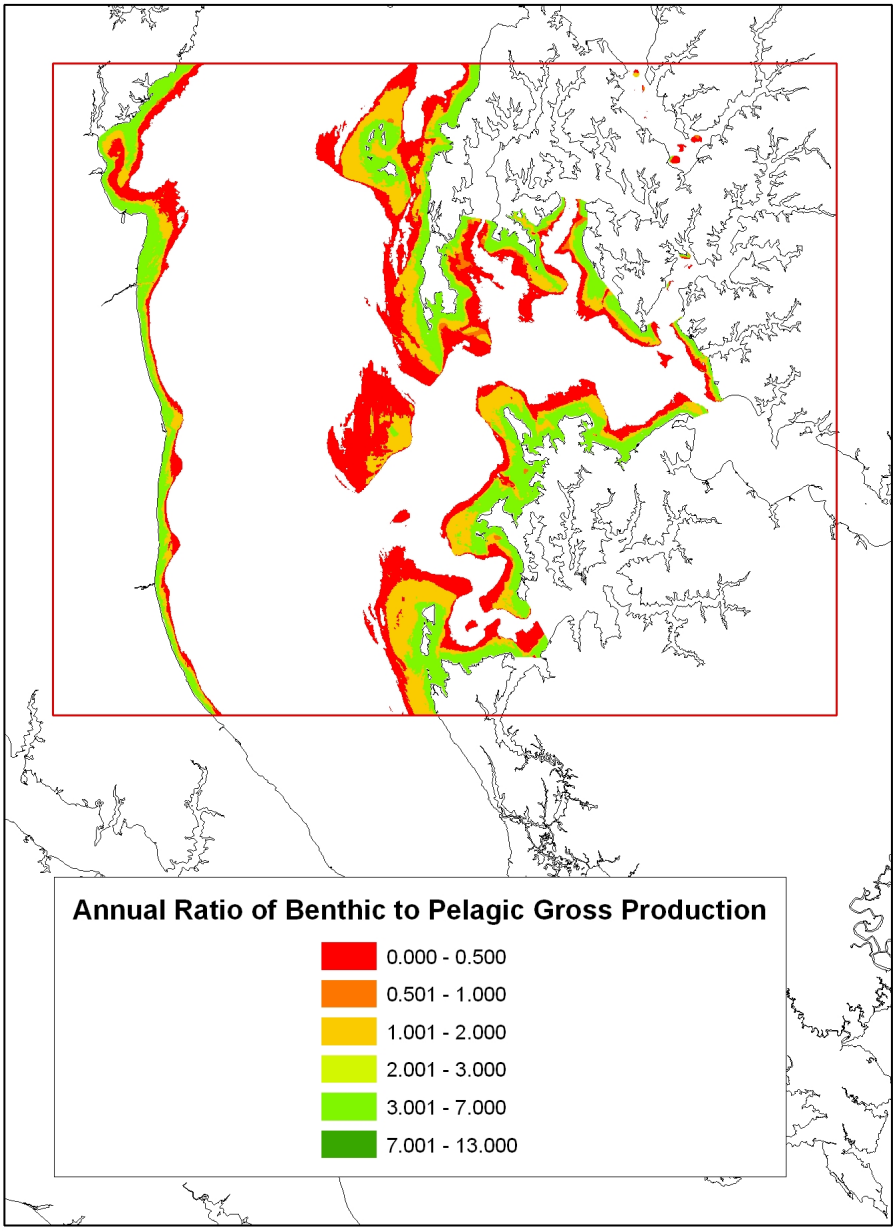

Figure 22. Ratio of benthic to pelagic production in the area represented by the red box.

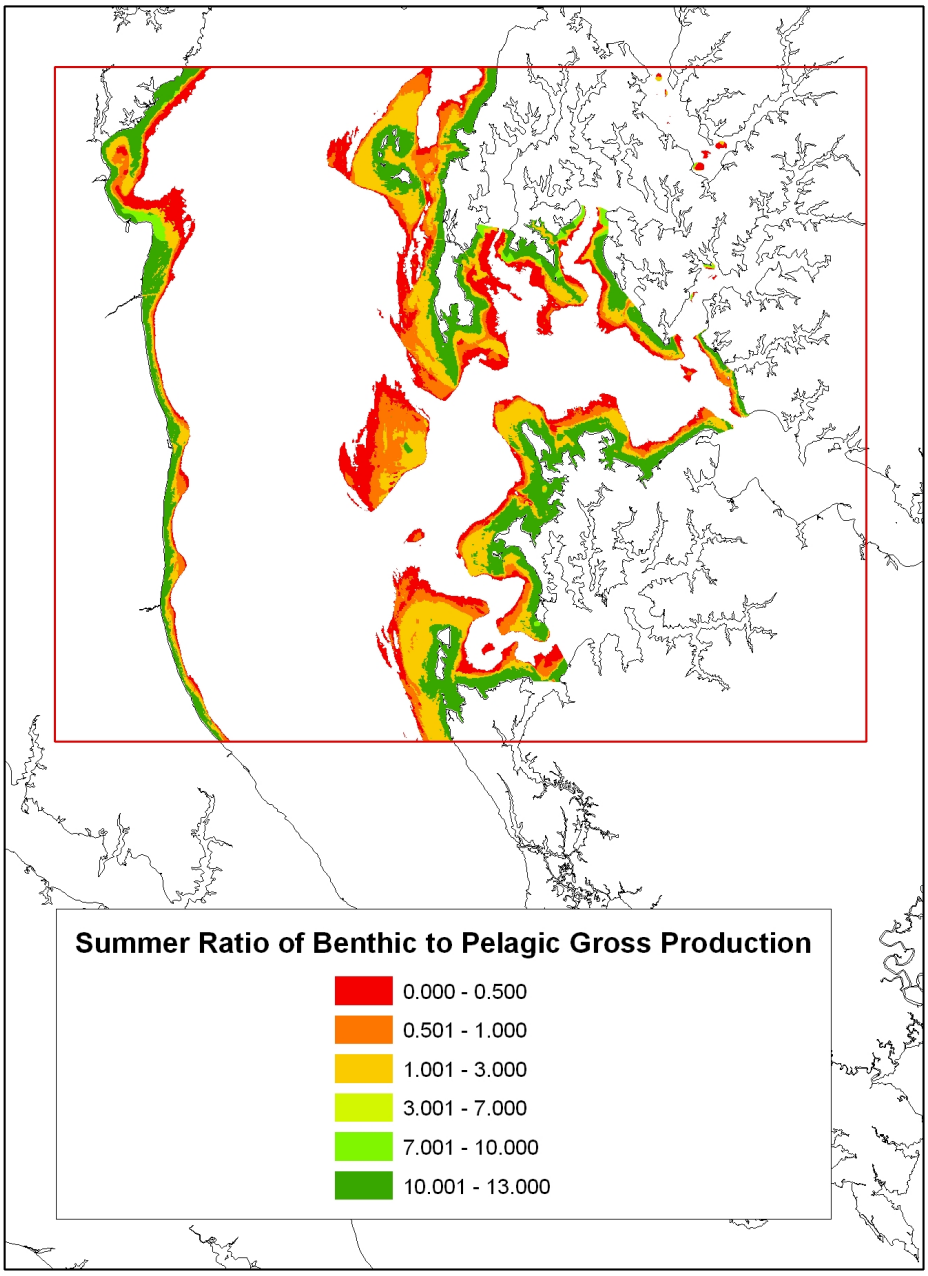

Figure 23. Ratio of average annual net pelagic over net benthic production, only a few scattered spots are expected to have a higher benthic than pelagic production.

Conclusions

Estimating MPB productivity presents a number of difficulties as it is characterized by high spatial and temporal variability. Fear et al.'s (2004) study related the euphotic area and production to the light field; these kinds of predictions could not be made without taking into account the bathymetry. However, this study measured multiple factors and attempted to correlate them to benthic O_2 production. The Fear et al. (2004) paper used the relationship between irradiance and production to estimate a shifting compensation depth in the Neuse River Estuary using bathymetry. By trading depth as a proxy for irradiance in this study, we develop seasonally specific relationships that can be applied to similar data for sediment grain size and bathymetry. However, the utilization of our numerical relationships in new environments might be difficult as this requires the validation of the model coefficients in the new system.

GIS mapping allowed for estimation of an environmental attribute over a spatial scale using variables to predict the attributes value. The precision of the estimation depends on the resolution of the measurement of the variables and the strength of the relationship between the variables and the attribute of interest. In this case, the variables were depth and sediment type. The spatial approach provided an advantage over studies which provide extrapolation by multiplying an attribute by area to provide a spatially adjusted value. ArcMap allows this same extrapolation but enables the estimated value to be modified by local variables which may provide more insight into specific locations.

High levels of spatial and temporal variability in the biomass and productivity of benthic microalgae often present difficulties in drawing broad conclusions regarding their dynamics (Rizzo et al. 1985; MacIntyre et al. 1996). In this study, benthic microalgal production was examined under different seasonal and spatial conditions. Cores were incubated *in vitro* at fixed PAR levels, and flux rates were measured from concentration time courses. This approach has yielded a number of environmental snapshots, but this approach is limited in that it does not account for subtle short-term environmental changes such as short-term variation in nutrient inputs, illumination, or grazing. Because of such variable conditions, MPB production may have a high temporal variability. Regardless of these sampling errors, MPB oxygen dynamics have been examined in a variety of systems (e.g. Fear et al. 2004; Reay et al. 1995; Murray & Wetzel 1987; Moncrieff et al. 1992; Sundback et al 2000).

Another potential limitation is the inability to exactly match *in vitr*o irradiance to *in situ* irradiance. In some cases *in situ* irradiance was much higher than could be reproduced in the lab (maximum laboratory irradiance 300 μmol photons m^{-2} s^{-1}). Previous studies have suggested that microphytobenthos photosynthesis reaches saturation between 30-360 μmol photons m^{-2} s^{-1} (MacIntyre et al.1996: Davis and MacIntyre 1983), and the highest PAR used in this study should have nearly saturated photosynthetic rates. The utility of these measurements is greatest when MPB productivity can be related to a contiguous measurable attribute (Table 5). Strong significant relationships exist in summer and winter between gross O_2 production and both PAR and percent sand, and between Net O_2 production PAR and percent sand.

Irradiance has been shown to be the primary factor behind MPB abundance and productivity in many different environments (MacIntyre et al. 1996) and sandy environments have been shown to have a positive effect on MPB chl *a* (Rizzo et al. 1985; MacIntyre et al. 1996 and references therein).

This study demonstrates that there are dramatic differences in MPB primary productivity between seasons in the Chesapeake Bay. It also demonstrates that sediment type and bathymetry can be correlated with benthic primary productivity. We have also provided an estimate that MPB contributes approximately 12% of total primary productivity in the Bay.

The reliability of the predicted primary production rates in this study can be gauged by the relative r^2's of each predictive equation as shown in Figure 17. The r^2 represents the fraction of variability that can be explained by the regression relationship. In most cases our predictive power is between 0.27 and 0.77, with the highest r^2's during the winter. Since the majority of these predictions can only estimate 50% of the variability in these rates, there are other factors which contribute to MPB dynamics, such as changes in predation from meiofauna, sediment resuspension events, and shading could account for much this unexplained variability.

MPB are an important component of primary production in the Chesapeake Bay. As SAV has dramatically reduced its distribution in the Bay's shallows, MPB importance as a link between nutrients and higher trophic levels has become more critical. As benthic primary producers, MPB play an important role in the transference of nutrients to higher trophic levels. By obtaining a ratio of their primary production with respect to total primary production in the Bay, we have more

insight as to the benthic contribution to Chesapeake Bay nutrient cycling. By inference, we can now conjecture that 12% of total primary production is made available to bottom-feeding mesofauna as MPB provide a primary food source for snails, nematodes, and crustaceans (Pinckney et al. 2003, Montagna 1984, Moncrief and Sullivan 2001). This may have implications for mesofauna habitat as MPB, their food source, is limited in abundance to 0-3 meters in depth. In addition, MPB biomass and primary productivity shifts with season which may further impact mesofauna populations

As benthic light conditions continue to deteriorate in the Bay, photosynthetic communities with a flexible survival strategy will have a distinct advantage in the light-limiting environment. MPB, with its high growth rate and potential for colonization is a logical successor to macrophytic benthic primary production whose dominance depended on low light attenuation in the water column.

Recommendations

It is critical in studies that attempt to predict an attribute over a spatial field that the temporal and spatial resolution of the data is adequate to provide confidence in the measurement. This is especially pertinent in studies that attempt to measure MPB which have high temporal and spatial variability. While this study involved over 200 cores and over 3000 analytical samples it was still questionable where it adequately characterized the dynamics of MPB. At the Horn Point site, only 7 days out of a total of 515 were sampled, which allows enormous quantities of temporal

variability to have been unmeasured. Thus, it may be advisable to focus on a single site to achieve as much spatial and temporal resolution as possible.

The r^2 values from the regressions were affected by the choice of sampling site. LTC and FB were very different environments than the HP site. As a result, any correlation which included measurements from all three sites would have a high variance. These divergent sites were chosen because they represented a wide range of MPB habitats in the Chesapeake Bay and together they would better represent the Bay as whole. A higher r^2 could have been achieved by choosing sites with more uniform light conditions and sediments but at the cost of representation. If this experiment were repeated it may prove advantageous to sample from similar locations.

As mentioned previously the maximum irradiance attainable in the laboratory incubations was 300 μmol m^{-2} s^{-1}, but we observed that higher irradiances produced higher rates of photosynthesis. Thus, there may be significant advantages in incubations performed in a natural light regime as demonstrated by the high O_2 flux from the initial HP sampling date (Figure 5). For future studies, it would be ideal if irradiances over 600 μmol m^{-2} s^{-1} could be achieved with better equipment in the environmental chamber.

In order to provide more temporal resolution it would have been worthwhile to eliminate depth replication and to incubate singles cores from each depth along with a core-water blank. This would have reduced the analytic load and enabled a better measure of the highly variable MPB abundance. In addition, it would have

been ideal to have at least 3 sampling dates per month to better represent MPB abundance and production.

A further improvement to this model could be the inclusion areas of known SAV abundance in the ArcMap extrapolation. Chesapeake Bay maps exist which show areas of known SAV abundance. In these areas, predicted MPB production could be multiplied by a constant to indicate the competitive relationship of SAV and MPB. Adjusting for this new type of bathymetry cover would not require new flux data, but only spatial information about the distribution of SAV and expertise on how to model its production with respect to total bay primary production. While this would make the model more complex, it would also account for the effects of macrophyte dominance in these areas.

Appendix I. Core data from all sites.

Depth Class	Site	Julian Date	Net daily O2	daily resp	gross daily	Depth	Chl *a*	Percent Sand	Surface PAR	Bottom PAR	ChamberPAR	*k*
shallow	HP	158	47.28	-45.27	92.55	0.56	59.36	96.36	1050	615	615.00	0.4185
		158	68.50	-53.99	122.49	0.56	63.73	96.36	1050	615	615.00	0.4185
		158	82.98	-61.75	144.73	0.56	46.33	96.36	1050	615	615.00	0.4185
Mid	HP	158	38.51	-32.82	71.32	0.80	46.33	97.12	1175	340	340	0.62
		158	36.00	-58.31	94.31	0.80	81.50	97.12	1175	340	340	0.62
		158	37.55	-38.10	75.65	0.80	104.46	97.12	1175	340	340	0.62
Deep	HP	158	-25.01	-33.64	8.62	2.22	5.71	92.25	1550	89	89	0.55898
		158	-32.19	-44.17	11.98	2.22	1.96	92.25	1550	89	89	0.55898
		158	-14.50	-53.63	39.13	2.22	6.20	92.25	1550	89	89	0.55898
shallow	HP2	205	47.69	-13.76	61.45	0.54		96.36	1494	303.7	300.00	1.3838
		205	48.50	-30.91	79.42	0.54	159.99	96.36	1494	303.7	300.00	1.3838
		205	48.58	-18.28	66.86	0.54	43.71	96.36	1494	303.7	300.00	1.3838
Mid	HP2	205	14.31	-8.75	23.06	1.04	6.08	97.12	1440	100	100	1.158
		205	11.42	-11.68	23.10	1.04	11.77	97.12	1440	100	100	1.158
		205	15.60	-2.01	17.61	1.04	23.61	97.12	1440	100	100	1.158
Deep	HP2	205	-16.76	-17.59	0.83	2.99	1.70	92.25	1400	3.5	3.5	1.0848
		205	-18.46	-15.95	-2.50	2.99	2.86	92.25	1400	3.5	3.5	1.0848
		205	-18.82	-26.14	7.32	2.99	5.51	92.25	1400	3.5	3.5	1.0848
shallow	HP3	319	-16.03	-27.68	11.65	0.68	95.46	96.36	300	130	130	0.399
		319	-2.42	-20.77	18.36	0.68	76.37	96.36	300	130	130	0.399
		319	-6.82	-24.06	17.24	0.68	86.83	96.36	300	130	130	0.399
Mid	HP3	319	-12.82	-22.14	9.32	1.43	31.32	97.12	500	20	100	0.8737
		319	-7.78	-21.33	13.55	1.43	37.88	97.12	500	20	100	0.8737
		319	-6.27	-19.81	13.54	1.43	29.63	97.12	500	20	100	0.8737
Deep	HP3	319	-11.10	-19.16	8.06	2.22	20.66	92.25	230	25	25	0.401578
		319	-9.72	-16.78	7.06	2.22	30.63	92.25	230	25	25	0.401578
		319	-13.20	-26.70	13.50	2.22	25.60	92.25	230	25	25	0.401578
shallow	HP4	24	1.59	-2.83	4.42	0.61	97.62	96.36	130	100	25	0.0854
		24	6.46	-6.22	12.68	0.61	65.83	96.36	130	100	25	0.0854
		24	14.06	-6.55	20.62	0.61	109.26	96.36	130	100	25	0.0854
Mid	HP4	24	1.29	-5.84	7.14	1.36	31.04	97.12	750	90	90	0.6138
		24	9.87	-5.69	15.56	1.36	53.98	97.12	750	90	90	0.6138
		24	10.63	-5.55	16.18	1.36	47.66	97.12	750	90	90	0.6138
Deep	HP4	24	-1.91	-9.63	7.71	2.21	39.60	92.25	850	25	100	0.6516
		24	-3.67	-11.55	7.88	2.21	32.40	92.25	850	25	100	0.6516
		24	-3.99	-8.44	4.45	2.21	25.58	92.25	850	25	100	0.6516
shallow	HP5	67	15.98	-15.78	31.75	0.30	138.03	96.36	1200	250	250	1.3624
		67	28.23	-16.12	44.34	0.30	188.30	96.36	1200	250	250	1.3624
		67	22.75	-15.10	37.85	0.30	163.59	96.36	1200	250	250	1.3624
Mid	HP5	67	13.26	-11.30	24.56	1.50	60.44	97.12	1200	170	170	1.4428
		67	22.98	-12.69	35.67	1.50	84.65	97.12	1200	170	170	1.4428
		67	15.07	-6.97	22.05	1.50	74.86	97.12	1200	170	170	1.4428
Deep	HP5	67	-7.74	-14.53	6.79	2.30	29.09	92.25	1300	80	80	0.4843
		67	-3.27	-13.01	9.75	2.30	43.48	92.25	1300	80	80	0.4843
		67	-0.54	-11.24	10.69	2.30	27.70	92.25	1300	80	80	0.4843

Deepest	HP5	67	-15.64	-15.02	-0.62	7.60		96.36	1160	1	1	0.4032
		67	-12.55	-13.76	1.20	7.60		96.36	1160	1	1	0.4032
		67	-13.90	-14.55	0.65	7.60		96.36	1160	1	1	0.4032
shallow	HP6	129	-11.22	-35.51	24.29	0.48	199.39	97.12	1500	900	300.00	0.3697
		129	-2.64	-32.65	30.01	0.48	190.17	97.12	1500	900	300.00	0.3697
		129	-2.30	-35.39	33.08	0.48	208.28	97.12	1500	900	300.00	0.3697
Mid	HP6	129	11.28	-33.62	44.90	1.48	123.83	92.25	1500	300	300	1.1183
		129	5.31	-37.13	42.44	1.48	128.97	92.25	1500	300	300	1.1183
		129	27.19	-37.45	64.64	1.48	115.85	92.25	1500	300	300	1.1183
Deep	HP6	129	-16.45	-17.10	0.65	2.48	23.18	96.36	1500	60	60	0.537
		129	-24.30	-25.31	1.01	2.48	9.93	96.36	1500	60	60	0.537
		129	-28.42	-33.87	5.45	2.48	18.32	96.36	1500	60	60	0.537
Deepest	HP6	129	-39.70	-47.10	7.40	7.70		97.12	1500	0.5	0.5	0.448
		129	-35.72	-44.61	8.89	7.70		97.12	1500	0.5	0.5	0.448
		129	-49.40	-59.04	9.64	7.70		97.12	1500	0.5	0.5	0.448
shallow	HP7	181	3.49	-35.74	39.24	0.67	101.12	92.25	1580	200	200	1.0686
		181	40.57	-29.32	69.90	0.67	118.99	92.25	1580	200	200	1.0686
		181	58.53	-23.99	82.53	0.67	134.80	92.25	1580	200	200	1.0686
Mid	HP7	181	0.09	-29.78	29.87	1.53	51.91	96.36	750	70	70	0.6866
		181	19.16	-33.02	52.17	1.53	72.81	96.36	750	70	70	0.6866
		181	10.18	-25.21	35.39	1.53	37.76	96.36	750	70	70	0.6866
Deep	HP7	181	-12.26	-15.50	3.24	2.63	9.25	97.12	650	15	15	0.6062
		181	-15.97	-18.91	2.94	2.63	6.47	97.12	650	15	15	0.6062
		181	-7.43	-21.42	13.99	2.63	14.38	97.12	650	15	15	0.6062
Deepest	HP7	181	-76.69	-88.59	11.90	7.70	3.74	92.25	1500	1	0	0.41247
		181	-58.78	-85.48	26.70	7.70	6.45	92.25	1500	1	0	0.41247
		181	-77.75	-87.83	10.08	7.70	7.02	92.25	1500	1	0	0.41247
Shallow	LTC	215	-27.11	-21.10	-6.01	0.78	2.36	24.37	1407	104	104	1.845
		215	-11.03	-29.53	18.49	0.78	2.08	24.37	1407	104	104	1.845
		215	-19.41	-38.66	19.25	0.78	3.52	24.37	1407	104	104	1.845
Mid	LTC	215	-24.80	-36.04	11.24	1.06	3.00	9.94	1458	90	90	1.3439
		215	-13.65	-17.65	4.01	1.06	1.98	9.94	1458	90	90	1.3439
		215	-7.34	-12.33	4.99	1.06	2.22	9.94	1458	90	90	1.3439
Deep	LTC	215	-22.03	-26.97	4.94	1.78	4.11	20.99	1550	10	10	1.352
		215	-17.13	-21.56	4.43	1.78	1.52	20.99	1550	10	10	1.352
		215	-23.50	-32.71	9.21	1.78	3.29	20.99	1550	10	10	1.352
Shallow	LTC 2	38	-8.53	-15.13	6.60	0.86	26.86	24.37	1100	300	300	0.7053
		38	-6.95	-11.07	4.12	0.86	19.82	24.37	1100	300	300	0.7053
		38	-11.26	-18.17	6.91	0.86	41.97	24.37	1100	300	300	0.7053
Mid	LTC 2	38	-13.88	-23.79	9.90	1.16	16.64	9.94	1000	150	150	0.749
		38	-18.42	-26.57	8.15	1.16	15.02	9.94	1000	150	150	0.749
		38	-18.79	-26.98	8.18	1.16	11.73	9.94	1000	150	150	0.749
Deep	LTC 2	38	-13.37	-16.55	3.18	1.96	12.22	20.99	1100	120	120	0.5064
		38	-12.46	-17.85	5.39	1.96	7.61	20.99	1100	120	120	0.5064
		38	-10.08	-15.86	5.78	1.96	12.20	20.99	1100	120	120	0.5064
Shallow	LTC 3	158	-19.33	-16.04	-3.28	0.76	9.43	24.37	800	100	100	1.29
		158	-24.68	-41.38	16.70	0.76	10.93	24.37	800	100	100	1.29
		158	-31.77	-47.73	15.96	0.76	12.27	24.37	800	100	100	1.29
Mid	LTC 3	158	-47.84	-62.21	14.38	1.16	14.80	9.94	1400	100	100	1.0419
		158	-44.95	-55.83	10.88	1.16	18.49	9.94	1400	100	100	1.0419

		158	-46.29	-61.68	15.39	1.16	11.55	9.94	1400	100	100	1.0419
Deep	LTC 3	158	-57.67	-90.09	32.42	1.76	8.82	20.99	1400	30	30	0.9817
		158	-58.89	-88.61	29.72	1.76	7.71	20.99	1400	30	30	0.9817
		158	-54.27	-92.64	38.37	1.76	10.99	20.99	1400	30	30	0.9817
Shallow	FB	228	-12.26	-14.37	2.11	0.64	14.85	na	150	2.5	0.6	2.9635
		228	-13.97	-17.33	3.36	0.64	8.22	na	150	2.5	0.6	2.9635
		228	-22.48	-28.48	6.00	0.64	10.85	na	150	2.5	0.6	2.9635
Mid	FB	228	-4.31	-2.22	-2.08	0.88	9.88	89.77	180	0.4	0.8	3.15858
		228	-10.87	-8.07	-2.80	0.88	6.67	89.77	180	0.4	0.8	3.15858
		228	-13.76	-17.09	3.33	0.88	10.98	89.77	180	0.4	0.8	3.15858
Deep	FB	228	-13.78	-12.82	-0.96	1.64	4.86	6.94	410	2.5	1.6	1.3842
		228	-31.68	-54.88	23.20	1.64	3.55	6.94	410	2.5	1.6	1.3842
		228	-18.01	-27.76	9.76	1.64	3.17	6.94	410	2.5	1.6	1.3842
Shallow	FB2	89	-4.94	-8.35	3.41	0.35	9.83	na	1450	400	300.00	1.2429
		89	-7.54	-19.50	11.96	0.35	7.42	na	1450	400	300.00	1.2429
		89	-2.05	-12.77	10.72	0.35	7.01	na	1450	400	300.00	1.2429
Mid	FB2	89	-9.35	-12.70	3.35	0.90	1.45	89.77	1496	85	85	1.2455
		89	-10.86	-14.18	3.31	0.90	2.58	89.77	1496	85	85	1.2455
		89	-11.28	-14.75	3.47	0.90	2.06	89.77	1496	85	85	1.2455
Deep	FB2	89	-11.16	-14.63	3.47	1.10	4.07	6.94	1495	46	46	1.2599
		89	-10.20	-13.10	2.89	1.10	2.89	6.94	1495	46	46	1.2599
		89	-12.28	-16.93	4.66	1.10	2.58	6.94	1495	46	46	1.2599
Shallow	FB3	214	-10.01	-69.83	59.81	0.56	13.63	na	750	125	125	1.297
		214	-19.74	-67.09	47.35	0.56	12.52	na	750	125	125	1.297
		214	-7.99	-38.34	30.35	0.56	13.63	na	750	125	125	1.297
Mid	FB3	214	-35.74	-51.48	15.73	1.01	6.07	89.77	750	15	15	1.6989
		214	-30.93	-36.90	5.97	1.01	8.90	89.77	750	15	15	1.6989
		214	-40.56	-57.14	16.58	1.01	10.28	89.77	750	15	15	1.6989
Deep	FB3	214	-31.14	-28.08	-3.06	1.24	4.54	6.94	750	7	7	1.6503
		214	-39.95	-50.21	10.25	1.24	9.95	6.94	750	7	7	1.6503
		214	-51.74	-76.95	25.22	1.24	6.48	6.94	750	7	7	1.6503

References

An S and Joye SB. (2001). Enhancement of coupled denitrification by benthic photosynthesis in shallow subtidal estuarine sediments. Limnology and Oceanography **46**: 62-74.

Coakley JP and Syvitski, JPM. (1991). Sedigraph technique. In: Principles of Grain-Size Analysis Chap 7. Ed. Syvitski Cambridge University Press.

Carman KR, Dobbs FC. (1997). Response of a benthic food web to hydrocarbon contamination. Limnology and Oceanography. **42** (3): 561-571.

Cahoon, LB. (1999). The role of benthic microalgae in neritic ecosystems. Oceanogr. Marine Biology Annual Review **37**: 47– 86.

Cooper, SR. (1995). Chesapeake Bay watershed historical land use: impact on water quality and diatom communities. Ecological Applications **5**(3):703-723.

Davis MW, McIntire CD. (1983). "Effects of Physical gradients on the production dynamics of sediment-associated algae." Marine Ecology Progress Series **13:** 103-114.

de Jonge VN (1990). Response of the Dutch Wadden Sea ecosystem to phosphorus discharges from the River Rhine. Hydrobiologia **195**:49–62

De Troch M, Cnudde C, Vyverman W, Vanreusel A. (2006). Increased production of faecal pelloets by the benthic harpacticoid Paramphiascella fulvofasciata: importance of the food source. **156** (3): 469-477.

Dyson KE, Bulling MT, Solan S, Hernandez-Milian G, Raffaelii DG, White PCL, Paterson DM. (2007). Influence of macrofaunal assemblages and environmental heterogeneity on microphytobenthic production in experimental systems. Proceedings of the Royal Society B **274**: 2547–2554.

Evrard V, Cook PLM, Veuger B, Huettel M, Middelburg JJ, (2008). Tracing carbon and nitrogen incorporation and pathways in the microbial community of a photic subtidal sand. Aquatic Microbial Ecology **53**: 257–269.

Facca C, Sfriso A, Socal G. (2002). Changes in abundance and composition of phytoplankton and microphytobenthos due to increased sediment fluxes in the Venice Lagoon, Italy. Estuarine, Coastal and Shelf Science **54**: 773-792.

Fattom A, Shilo M. (1984). Hydrophobicity as an adhesion mechanism of benthic cyanobacteria. Applied Environmental Microbiology. **47** (1): 135-143.

Fear J, Tom G, Hall N, Loftin J, Paerl H. (2004). Predicting benthic microalgal oxygen and nutrient flux responses to a nutrient reduction management strategy for the eutrophic Neuse River Estuary, North Carolina, USA." Estuarine, and Coastal Shelf Science **61:** 49-506.

Fisher TR, Hagy JD, Boynton WR, Williams MR. (2006). "Cultural eutrophications in the Choptank and Patuxent estuaries of Chesapeake Bay." Limnology and Oceanography **51** part2: 435-447.

Gallegos CL, Jordan TE (2002). Impact of the spring 2000 phytoplankton bloom in Chesapeake Bay on optical properties and light penetration in the Rhode River, Maryland. Estuaries **25**:508–518.

Hagy JD, Boynton WR, Keefe CW, Wood KV. (2004). Hypoxia in the Chesapeake Bay, 1950-2001: Long-term change in relation to nutrient loading and river flow. Estuaries **27**: (4) 634-658

Hansen JA, Alongi DM, Moriarty DJW, Pollard PC. (1987). "The Dynamics of Benthic Microbial coCommunities at Davies Reef, Central Great-Barrier-Reef." Coral Reefs: **6** (2) 63-70.

Harding LW, Mallonee ME, Perry ES. (2002). Toward a predictive understanding of primary productivity in a temperate, partially stratified estuary. Estuarine, Coastal and Shelf Science **55**: 437-463.

Holyoke RR. (2008). Biodeposition and biogeochemical processes in shallow, mesohaline sediment of Chesapeake Bay Ph.D. Thesis, UMCP.

Ichimi K, Tada K, Montani S. (2008). Simple estimation of penetration rate of light in intertidal sediments. Journal of Oceanography. **64**: 399-404.

Kana TM, Hunt CD, Oldham MD, Bennet GE, Cornwell JC. (1994). "Membrane inlet mass spectrometer for rapid high-precision determination of N_2, O_2, and Ar in environmental water samples." Analytical Chemistry **66**(23): 4166-4170.
Kana TM, Wiess DL. (2004). Comment on Comparison of isotope pairing and N_2:Ar methods for measuring sediment Denitrification. Estuaries **25**: 1077-1087

Kemp WM, Puskaric S, Faganeli A, Smith E, Boynton W (1999). Pelagic-benthic coupling and nutrient cycling. In: Malone T, Malej A, Harding L, Smodlaka N, Turner R (eds) Ecosystems at the land-sea margin: drainage basin to coastal sea. American Geophysical Union, Washington,DC, p295–339

Kemp WM, Boyton WR, Adolf JE, Boesch DF, Boicourt WC, Brush G, Cornwell JC, Fisher TR, Gilbert PM, Hagy JD, Hardin LW, Houde ED, Kimmel DG, Miller WD, Newel IE, Roman MR, Smith EM, Stevenson JC. (2005). "Eutrophication of

Chesapeake Bay: historical trends and ecological interactions." Marine Ecology Progress Series **303**: 1-29.

Lundkvist M, Gangelhof U, Lunding J, Flindt MR. (2007). Production and fate of extracellular polymeric substances produces by benthic diatoms and bacteria: A laboratory study. Estuarine Coastal and Shelf Science **75** (3): 337-346

Lee K-Y, Fisher TR, Jordan TE, Correl DL, and Weller DE. (2000). Modeling the hydrochemistry of the Choptank River basin using GWLF and Arc/Info: 1. Model calibration and validation. Biogeochemistry **49**: 143-173

MacIntyre HL, Cullen JJ. (1995). "Fine-scale vertical resolution of chlorophyll and photosynthetic parameters in shallow-water benthos." Marine Ecology Progress Series **122** (1-3) 227-237.

MacIntyre HL, RJ Geider and DC Miller (1996). "Microphytobenthos: the ecological role of the "secret garden" of unvegetated shallow-water marine habitats. I. Distribution, abundance, and primary production." Estuaries **19**(2a): 186 -201.

Madsen KN, Nilsson P, Sundback K. (1992). "The influence of benthic microalgae on the stability of a subtidal sediment." Journal of Experimental Biology and Ecology. **170** (2): 159-177.

Mallin MA, Burkholder JM, Sullivan MJ (1992) Contributions of Benthic microalgae to coastal fishery yield. Trans Am Fish Soc **121**:691–693

Meyercordy J, Meyer-Reil LA. (1999). "Primary Production of benthic microalgae in two shallow coastal lagoons of different tropic status in the southern Baltic Sea." Marine Ecology Progress Series **178**: 179-191.

Middelburg JJ. (2000). The fate of intertidal microphytobenthos carbon: an in situ ^{13}C-labeling study. Limnology and Oceanography **45**(6): 1224-1234.

Miles A, Sundback K (2000). "Diel variation in microbenthic productivity in areas of different tidal amplitude." Marine Ecology Progress Series **205**: 11-22.

Miller DC, Geider RJ, MacInytre HL. (1996). "Microphytobenthos: The ecological role of the "secret garden" of unvegetated shallow-water marine habitats. 2. Role in sedimentary sability and shallow-water food webs." Estuaries **19** (2A): 202-212.

Montagna, PA, (1984). In situ measurement of meiobenthic grazing rates on sediment bacteria and edaphic diatoms. Marine Ecology Progress Series **8**: 119- 130.

Moncrieff CA, Sullivan MJ, Daehnick AE. (1992). "Primary production dynamics in sea grass bends of Missisipi Sound the contributions of seagrass, epiphytic algae,

sand microlfora and phytoplankton." Marine Ecology-Progress Series. **87** (1-2): 161-171.

Moncreiff CA, Sullivan MJ (2001). Trophic importance of epiphytic algae in subtropical seagrass beds: evidence from multiple stable isotope analyses. Marine Ecology Progress Series **215**: 93–106.

Murray, L and RL Wetzel. (1987). "Oxygen production and consumption associated with the major autotrophic groups in two temperate seagrass communities." Marine Ecology Progress Series **38**: 231-239.

Owens, MS (2009). Nitrogen cycling and controls on denitrification in mesoahaline sediment of Chesapeake Bay. M.S. Thesis. MEES Program, University of Maryland.

Pinckney J, Paerl HW,Fitzpatrick M. (1995). "Impacts of seasonality and nutrients on microbial mat community structure and function." Marine Ecology Progress Series **123**: 207-216.

Pinckney JL, Carman KR, Lumsden SE, Hymel SN. (2003). Microalgal - meiofaunal trophic relationships in muddy, intertidal estuarine sediments. Aquatic Microbial Ecology **31**:99-108.

Pollard PC, Kogure K. (1993). Bacterial decomposition of detritus in a tropical seagrass (*Syringodium isoetifolium*) eco-. system, measured with [Methyl-H]thymidine. Aust. Journal of Marine Freshwater Restoration **44**: 155–172

Rasmussen MB, Henriksen K, Jensen A. (1983). "Possible causes of temporal fluctuations in primary production of the microphytobenthose in the Danish Wadden Sea." Marine Biology **73** (2): 109-114.

Risgaard-Petersen N. (2003). Coupled nitrification-denitrification in autotrophic and heterotrophic estuarine sediments: on the influence of benthic microalgae. Limnology and Oceanography. **48**: 93–105.

Reay WG, Gallagher DL, Simmons GM. (1995). "Sediment-water column oxygen and nutrient fluxes in nearshore environments of the Lower Delmarva Peninsula, USA." Marine Ecology-Progress Series. **118** (1-3): 215-227.

Rizzo WM, and RL Wetzel. (1985). Intertidal and shoal benthic community metabolism in a temperate estuary: Studies of spatial and temporal scales of variability. Estuaries **8**: 342-351.

Rizzo WM. (1990). Nutrient exchanges between the water column and a subtidal benthic microalgal community. Estuaries **13**:219-226.

Sundback K, A Miles and Eoransson (2000). "Nitrogen fluxes, denitrification and

the role of microphytobenthos in microtidal shallow-water sediments: an annual study." Marine Ecology Progress Series **200**: 59-76.

Sundback K. (2007). Impact of biodeposition on macrofaunal communities in intertidal sandflats. Marine Ecology. **17** (1-3) 159-174.

Sullivan MJ, Moncreif CA. (1990). Edaphic algae are important component of salt marsh food webs: evidence from multi stable isotope analysis. Marine Ecology Progress Series **121**:99–116.

Rivkin RB, Putt M. (1987). "Photosynthesis and cell-division by Antarctic microalgae-comparison of benthic, planktonic, and ice alage." Journal of Phycology **23** (2): 223-229.

Van Heukelem L, Lewitus AJ, Kana TM, Craft NE. (1994) Improved separations of phytoplankton pigments using temperature-controlled high performance liquid chromatography. Marine Ecology Progress Series **114**: 303-313.

Varela M, Penas E. (1985). Primary production of benthic microalgae in an intertidal sand flat of the Ria de Arosa, NW Spain. Marine Ecology Progress Series **25**: 111 – 119.

Yallop ML, Dewinder B, Paterson DM. (1994). Comparative structure, primary production and biogenic stabilization of cohesive and noncohesive marin-sediments inhabited by microphytobenthos. Estuarine Coastal and Shelf Science. **39** (6): 565-582.